APPROVED FOR PUBLIC RELEASE, DISTRIBUTION UNLIMITED

ALEX(02)-TR-75-02-PART B

AFOSR - TR - 76 - 1064

3

COUNTER''ASION STUDIES
THE EFFECTS OF NOISE, DISSIMILARITY, AND PREFILTERING ON CEPSTRUM ANALYSIS

SEMI-ANNUAL TECHNICAL REPORT NO. 5-PART B
1 MAY 1975 TO 31 OCTOBER 1975

Prepared by
David Sun

TEXAS INSTRUMENTS INCORPORATED
Equipment Group
Post Office Box 6015
Dallas, Texas 752'

ADA029560

DDC
SEP 13 1976
B

Contract No. F44620-73-C-0055
Amount of Contract: $294,749
Beginning 23 April 1973
Ending 30 June 1976

Prepared for

AIR FORCE OFFICE OF SCIENTIFIC RESEARCH

Sponsored by

ADVANCED RESEARCH PROJECTS AGENCY
Nuclear Monitoring Research Office
ARPA Program Code No. F10
ARPA Order No. 1827

30 November 1975

Acknowledgment: This research was supported by the Advanced Research Projects Agency, Nuclear Monitoring Research Office, under Project VELA-UNIFORM, and accomplished under the direction of the Air Force Office of Scientific Research under Contract Number F44620-73-C-0055.

APPROVED FOR PUBLIC RELEASE, DISTRIBUTION UNLIMITED

ALEX(02)-TR-75-02-PART B

COUNTEREVASION STUDIES
THE EFFECTS OF NOISE, DISSIMILARITY, AND PREFILTERING ON CEPSTRUM ANALYSIS

SEMI-ANNUAL TECHNICAL REPORT NO. 5-PART B
1 MAY 1975 TO 31 OCTOBER 1975

Prepared by
David Sun

TEXAS INSTRUMENTS INCORPORATED
Equipment Group
Post Office Box 6015
Dallas, Texas 75222

ACCESSION for		
NTIS	White Section	☑
DDC	Buff Section	☐
UNANNOUNCED		☐
JUSTIFICATION		
BY		
DISTRIBUTION/AVAILABILITY CODES		
Dist.	AVAIL. and/or SPECIAL	
A		

Contract No. F44620-73-C-0055
Amount of Contract: $294,749
Beginning 23 April 1973
Ending 30 June 1976

Prepared for

AIR FORCE OFFICE OF SCIENTIFIC RESEARCH

Sponsored by

ADVANCED RESEARCH PROJECTS AGENCY
Nuclear Monitoring Research Office
ARPA Program Code No. F10
ARPA Order No. 1827

30 November 1975

Acknowledgment: This research was supported by the Advanced Research Projects Agency, Nuclear Monitoring Research Office, under Project VELA-UNIFORM, and accomplished under the direction of the Air Force Office of Scientific Research under Contract Number F44620-73-C-0055.

ABSTRACT

The effects of the noise, the dissimilarity, and the prefiltering on the detection of the P-pP delay time and the successful decomposition of the mixed P- and -pP wave by employing the cepstrum analysis are studied here. These effects have been investigated by extracting the direct P-phases and the surface reflected pP-phases from several presumed underground explosions in eastern Kazakh, and remixing them at various time delays with the addition of various levels of the realistic seismic noise. The quality of the cepstrum analyzed results as a function of the signal-to-noise ratio, the delay time, and the dissimilarity between the P-phase and the pP-phase have been obtained for a number of such events. In general, it is found that the cepstrum analysis can detect the P-pP delay time as short as 0.4 second and successfully recover the P- and the pP-phases for the signal-to-noise ratio down to about 12 dB. When the similarity coefficient between the P- and the pP-phases is less than 1.0, the detection of the P-pP delay time becomes not so obvious as it is when they are identical. The dissimilarity between the P-phase and the pP-phase will affect the detection of the P-pP delay time more seriously than the noise in the cepstrum analysis. Prefiltering of the noisy mixed P- and -pP wave with the standard bandpass filter will not affect the cepstrum analyzed results as long as the filter band covers the entire signal spectrum; although it seems that no prefiltering will offer better detection of the P-pP delay time.

PRECEDING PAGE BLANK-NOT FILMED

ACKNOWLEDGMENTS

The author is grateful to Lawrence S. Turnbull, Jr. for reviewing the manuscript, to Stephen S. Lane for his technical comments, and to Cherylann B. Saunders for typing the manuscript.

TABLE OF CONTENTS

LIST OF FIGURES

LIST OF FIGURES
(continued)

LIST OF FIGURES
(continued)

LIST OF TABLES

SECTION I
INTRODUCTION

In the previous reports on cepstrum analysis (Lane and Sun, 1974a, 1974b, 1975), the noise was not taken into consideration explicitly, since we usually chose the signals with reasonably good signal-to-noise ratio in order not to complicate the problems of interest. Surprisingly, among the few published articles on the applications of the cepstrum analysis to seismology, there was only one occasion where the noise was discussed (Ulrych, 1971). Even so, it was only given as an example using randomly generated white noise instead of the real seismic noise associated with the signal, and the signal-to-noise ratio was quite fair (20 dB).

Just as in most signal processing problems, we can expect that noise will affect the capability of the cepstrum analysis on the detection of the P-pP delay time and the successful decomposition of the mixed P- and -pP wave. The questions to be asked are how, and to what degree, is the effect of the noise. The answers to these questions, together with the noise level at an observational array, can lead to more meaningful cepstrum analysis of low signal-to-noise ratio signals (which are usually associated with the low magnitude presumed nuclear explosions), and an estimate of the magnitude and depth at which these events might be concealed by overburying.

In addition to the effect of noise on the cepstrum analysis, the effect of dissimilarity between the P-phase and the pP-phase has also been investigated. The information obtained from the comparison between the two kinds of effects can be used to explain the cepstrum analyzed results for the naturally mixed P waves where the pP-phase usually can not be considered as the exact replica of the P-phase.

The signal and the noise estimates used in this study are taken from the teleseismic short-period P waves of presumed underground explosions in eastern Kazakh as recorded at NORSAR. Therefore, it will not be appropriate to generalize the experimental results in this report for some other class of signals and noise without due consideration.

In Section II, a theoretical discussion of these problems will be given. The experimental results using the synthetic data are presented in Section III. Finally, the results from the analysis of several naturally mixed P- and -pP waves with various signal-to-noise ratios are given in Section IV.

SECTION II

THEORETICAL CONSIDERATIONS

In this section, we look into the problem from the mathematical point of view. Although the derived equations for the complex cepstrum and the resolved signals can not be explicitly expressed as a function of the signal-to-noise ratio and the dissimilarity of the two signals, we can see from the equations where the noise and the dissimilarity enter into the problem.

A. THE EFFECT OF NOISE

Let us consider a mixed signal consisting of two identical signals with some additive noise as follows:

$$x(n) = s(n) + as(n-n_o) + \epsilon(n) \qquad \text{(II-1)}$$

where a is a scale constant, n_o is the time delay, and $\epsilon(n)$ is the additive noise. The equation (II-1) can be rearranged in the following form:

$$x(n) = s(n) * m(n) + \epsilon(n) \qquad \text{(II-2)}$$

where $m(n) = \delta(n) + a\delta(n-n_o)$ ($\delta(n)$ is the Dirac delta function) is the multipath operator which convolves with the signal.

The complex cepstrum of $x(n)$ is obtained by the forward cepstrum transformation as given below. First, take the z-transform of $x(n)$ as follows,

$$X(z) = S(z)\,(1 + az^{-n_o}) + E(z) \,, \qquad \text{(II-3)}$$

where $S(z)$ and $E(z)$ are the z-transforms of the signal and the noise, respectively. To obtain the complex cepstrum of $x(n)$, we have to take complex logarithm of equation (II-3) as follows:

$$\hat{X}(z) = \ell n\left[X(z)\right]$$

$$= \ell n\left[S(z)\right] + \ell n(1 + az^{-n_o}) + \ell n\left[1 + \frac{E(z)/S(z)}{1 + az^{-n_o}}\right]. \quad \text{(II-4)}$$

Now, if

$$\max_{-\pi<\omega<\pi} \left| ae^{-jn_o\omega} \right| < 1 ,$$

the complex cepstrum of $x(n)$ can be expressed in the following form:

$$\hat{x}(n) = \hat{s}(n) + \sum_{k=1} (-1)^{k+1} \frac{a^k}{k} \delta(n - kn_o)$$

$$+ \text{z-transform}^{-1}\left[\ell n\left(1 + \frac{E(z)/S(z)}{1 + az^{-n_o}}\right)\right] \quad \text{(II-5)}$$

where:

z-transform^{-1}[ ] stands for inverse z-transform

and

$\hat{s}(n)$ is the complex cepstrum of the signal.

In general the complex cepstrum of the noise, which is represented by the last term in equation (II-5) can be expected to spread over the entire cepstrum time. However, with good signal-to-noise ratio, the last term in equation (II-5) can be expected to be small and the cepstral peaks (at least the first few) of the multipath operator (which is the second term in equation (II-5)), should be readily identifiable. The appropriate comb filter, which eliminates the second term in equation (II-5), can be applied at the right cepstrum time, i.e., $n = kn_o$. Then the resolved signal, which is the inverse cepstrum transform of the filtered $\hat{x}(n)$, will be

$$\underset{\sim}{s}(n) = s(n) + \text{z-transform}^{-1}\left[\frac{E(z)}{1 + az^{-n_o}}\right]. \qquad \text{(II-6)}$$

Therefore, the additive noise in the input mixed signal $x(n)$ will show up in the resolved signal $\underset{\sim}{s}(n)$ as additive noise, which is the original noise filtered by the linear system corresponding to $(1 + az^{-n_o})^{-1}$.

From the expressions given in equations (II-5) and (II-6), it is hard to see explicitly the effect of the noise on the cepstrum analysis. That is, the explicit dependence of the detection of the cepstral peaks and the quality of the resolved signal on the signal-to-noise ratio can not be obtained analytically. Nevertheless, it is quite clear that the noise will definitely smear the cepstral peaks of the multipath operator, and the degree of the smear should depend on the signal-to-noise ratio.

B. THE EFFECT OF DISSIMILARITY

The dissimilarity here refers to the situation when the component signals which form the mixed signal are not identical. We may treat this case in the following noise-like analysis. Let the mixed signal be

$$x(n) = s_1(n) + s_2(n - n_o) \qquad \text{(II-7)}$$

where $s_1(n)$ and $s_2(n)$ are not identical. Proceeding as if this were a noise analysis, let

$$\epsilon_d(n) = s_2(n) - as_1(n) \qquad \text{(II-8)}$$

where a is a constant and can be uniquely determined by requiring that the quantity $\sum_n \left|\epsilon_d(n)\right|^2$ be a minimum. Then equation (II-7) can be rewritten as follows:

$$x(n) = s_1(n) + as_1(n-n_o) + \epsilon_d(n-n_o) . \qquad \text{(II-9)}$$

Comparing equations (II-9) and (II-1), it is plausible to treat the difference between the two component signals as the noise. We must keep in mind, though, that $\epsilon_d(n)$ is closely related to the signals $s_1(n)$ and $s_2(n)$. In general, this is not the case for the noise as discussed in Subsection A.

Following the same procedure used in Subsection A, the complex cepstrum of $x(n)$ can be found to be:

$$\hat{x}(n) = \hat{s}_1(n) + \sum_{k=1} (-1)^{k+1} \frac{a^k}{k} \delta(n-kn_o)$$

$$+ \text{ z-transform}^{-1}\left[\ell n\left(1 + \frac{E_d(z) z^{-n_o}/S_1(z)}{1 + az^{-n_o}}\right)\right] \qquad \text{(II-10)}$$

where $E_d(z)$ and $S_1(z)$ are the z-transforms of $\epsilon_d(z)$ and $s_1(n)$, respectively, and $\hat{s}_1(n)$ is the complex cepstrum of $s_1(n)$. Equation (II-10) is similar to equation (II-5), but now the last term in the equation is attributed to the fact that $s_1(n)$ and $s_2(n)$ are non-identical. Again, in general, we can expect that the last term will be non-zero for the entire cepstrum time domain. However, when $s_1(n)$ and $s_2(n)$ are similar $|\epsilon_d(n)|$ can be considered small as compared to $|s_1(n)|$ and $|s_2(n)|$. Then the last term in equation (II-10) can be expected to be small and the cepstral peaks of the multipath operator might be identified. The application of the appropriate comb filter to $\hat{x}(n)$ will yield the resolved signal

$$\underset{\sim}{s}_1(n) = s_1(n) + \text{z-transform}^{-1}\left[\frac{E_d(z)\, z^{-n_o}}{1 + az^{-n_o}}\right] . \qquad \text{(II-11)}$$

The estimate of the $s_2(n)$ will be

$$\underset{\sim}{s}_2(n) = x(n) - \underset{\sim}{s}_1(n)$$

$$= s_2(n-n_o) - \text{z-transform}^{-1}\left[\frac{E_d(z)\, z^{-n_o}}{1 + az^{-n_o}}\right] \qquad \text{(II-12)}$$

Thus, the dissimilarity of $s_1(n)$ and $s_2(n)$ will appear in the cepstrum resolved signals, $\underset{\sim}{s}_1(n)$ and $\underset{\sim}{s}_2(n)$, as the filtered additive noise.

From the above discussion, it seems that the noise and the dissimilarity will affect the cepstrum analysis in the similar fashion. In practice however, $\epsilon_d(n)$ in equation (II-8) can be expected to be correlated to the signal more than the noise $\epsilon(n)$ and the spectral content of $\epsilon_d(n)$ will be similar to that of the signal. Hence, the complex cepstrum attributed to $\epsilon_d(n)$, which is the last term in equation (II-10), might be distributed more in the same range where the signal lies than elsewhere along the cepstrum time axis. Therefore, it is conjectured that the dissimilarity might affect the detection of the cepstral peaks of the multipath operator more seriously than does the noise.

C. THE EFFECT OF PREFILTERING

For the noisy mixed signal as given in equation (II-1), intuitively, one would want to filter out part of the noise in the signal $x(n)$ to improve the signal-to-noise ratio. But the tradeoff in improving the signal-to-noise ratio usually is the signal distortion. In the cepstrum analysis, the signal distortion might make it harder to detect the cepstral peaks of the multipath operator.

The spectrum of the mixed signal $x(n)$ can be easily obtained by letting $z = e^{j\omega}$ in the equation (II-3)

$$X(\omega) = S(\omega)\, M(\omega) + E(\omega) \qquad \text{(II-13)}$$

where ω is the angular frequency and $j = \sqrt{-1}$. $S(\omega)$ is the spectrum of $s(n)$ and $M(\omega)$ is the spectrum of multipath operator $m(n)$, i. e.,

$$M(\omega) = (1 + ae^{-j\omega n_o}) .$$

Writing the spectrum in the polar form

$$X(\omega) = |A(\omega)| \; |M(\omega)| \; e^{j[\psi(\omega) + \phi(\omega)]} \tag{II-14}$$

where

$$A(\omega) = S(\omega) + \frac{E(\omega)}{1 + ae^{-j\omega n_o}} , \quad \psi(\omega) \text{ is the phase of } A(\omega),$$

$$|M(\omega)| = \sqrt{1 + a^2 + 2a \cos\omega n_o} , \quad \text{and}$$

$$\phi(\omega) = \tan^{-1} \frac{-a \sin\omega n_o}{1 + a \cos\omega n_o} .$$

Thus, in both the amplitude and the phase spectra of $x(n)$, the multipath operator $m(n)$ represents a periodic modulation whose period in the frequency domain is equal to the inverse of the delay time in $m(n)$. Figure II-1 shows the amplitude spectrum of $x(n)$ which will add in the understanding of the periodic modulation. By examining equations (II-13), (II-4), and (II-5), it is not hard to see that the cepstral peaks of the multipath operator, which is the second term in equation (II-5), are the direct result of the periodic modulation. Hence, it is understood that those ripples of the periodic modulation shown in Figure II-1 carry the essential information for the detection of the cepstral peaks.

Now, let us apply a standard bandpass filter to $X(\omega)$. The filter response is

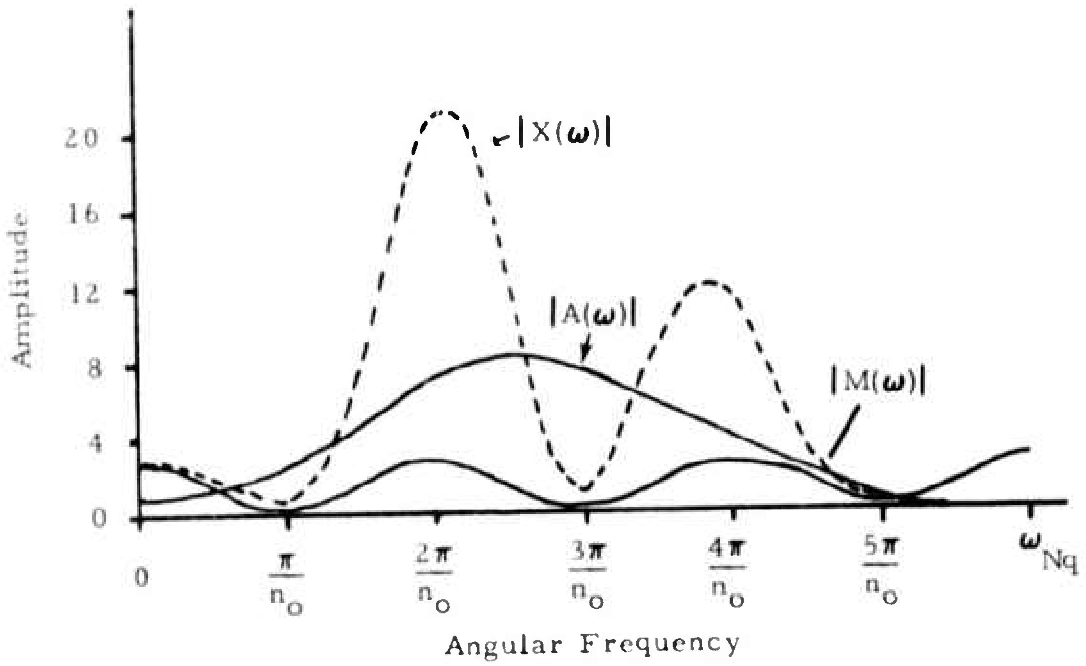

FIGURE II-1

AMPLITUDE SPECTRA OF $X(\omega)$, $A(\omega)$, AND $M(\omega)$

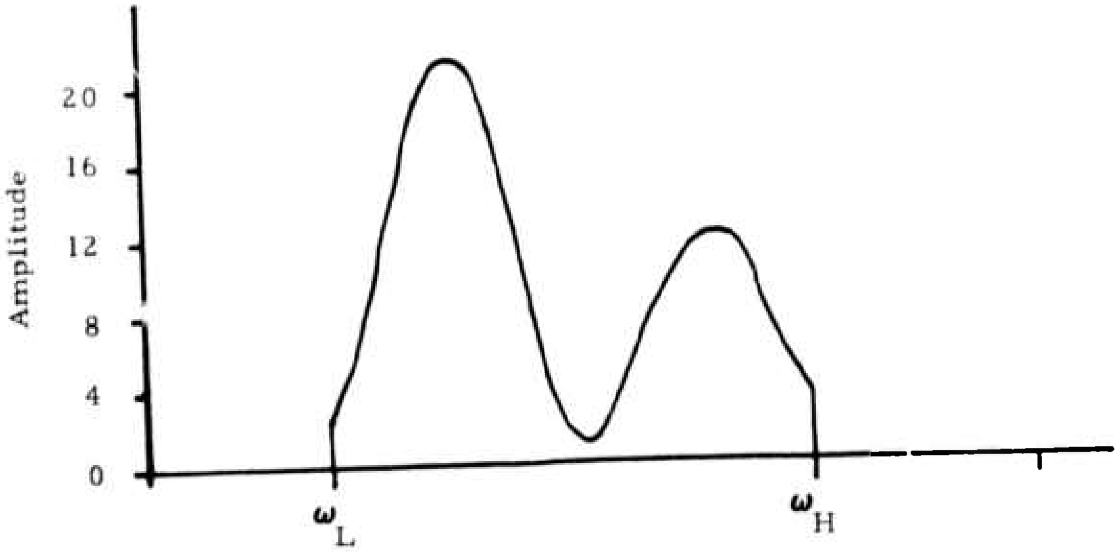

FIGURE II-2

FILTERED AMPLITUDE SPECTRA OF $X(\omega)$

$$A_B(\omega) = 1 \qquad \omega_L \leq \omega \leq \omega_H$$

$$A_B(\omega) = 0 \qquad \omega < \omega_L , \omega > \omega_H .$$

The filtered $X(\omega)$ is shown in Figure II-2. It is clear that we removed the spectra for $\omega < \omega_L$ and $\omega > \omega_H$, but we also removed the ripples in those frequency ranges. Thus, the periodicity of the amplitude modulation originally associated with $M(\omega)$ is destroyed. This, in turn, will affect the nice appearance of the cepstral peaks as predicted by the second term in equation (II-5). Therefore, it is reasonable to believe that any prefiltering technique which will destroy the periodicity of the amplitude modulation produced by the multipath operator will not help the cepstrum analysis for detection of the delay time.

SECTION III
EXPERIMENTAL RESULTS - SYNTHETIC SIGNALS

As pointed out in the previous section, from the mathematical expressions it is hard to see explicitly the effects of the noise, the dissimilarity, and the prefiltering. Therefore, to draw some practically useful conclusions about these effects, the most direct way is to cepstrum analyze a sufficient number of synthetic signals made from the class of signals in which we are interested. This section presents the experimental results to explicitly demonstrate these effects on the detection of the P-pP delay time and the successful decompositions of the mixed P- and -pP waves. These effects are treated separately in order to isolate one effect from the other for better demonstration. The class of signals which are used here are the teleseismic short-period P waves (with sampling rate of 10 samples per second) of the presumed underground explosions in the eastern Kazakh (EKAZ) recorded at NORSAR.

A. PREPARATION OF SYNTHETIC SIGNALS

First, four high signal-to-noise ratio EKAZ events, as listed in Table III-1, are cepstrum analyzed and successfully decomposed into their P-phases and pP-phases. Figure III-1 shows the typical result for KAZ/081/04N. The solid line is the resolved P-phase and the dashed line is the pP-phase. These resolved P-phases and pP-phases, together with the real seismic noise associated with them, are then used to construct the synthetic signals.

To study the effect of the noise, the synthetic signals are constructed as follows:

TABLE III-1

CEPSTRUM DECOMPOSITION OF FOUR EKAZ EVENTS

	Event I. D.	Date	Location: Latitude °N	Location: Longitude °E	m_b	Cepstrum Decomposition*
1	KAZ/081/04N	03-22-71	49.7	78.2	5.8	${}_1x(n) = {}_1s_p(n) + {}_1s_p p(n-6)$
2	KAZ/170/06N	06-19-71	50.0	77.7	5.5	${}_2x(n) = {}_2s_p(n) + {}_2s_p p(n-6)$
3	KAZ/282/06N	10-09-71	50.0	77.7	5.4	${}_3x(n) = {}_3s_p(n) + {}_3s_p p(n-5)$
4	EKZ/159/01N	06-07-71	49.8	78.2	5.5	${}_4x(n) = {}_4s_p(n) + {}_4s_p p(n-7)$

*

${}_ix(n)$: the time trace of the event i

${}_is_p(n)$: cepstrum resolved P-phase

${}_is_p p(n-n_o)$: cepstrum resolved pP-phase

n_o : P-pP delay time.

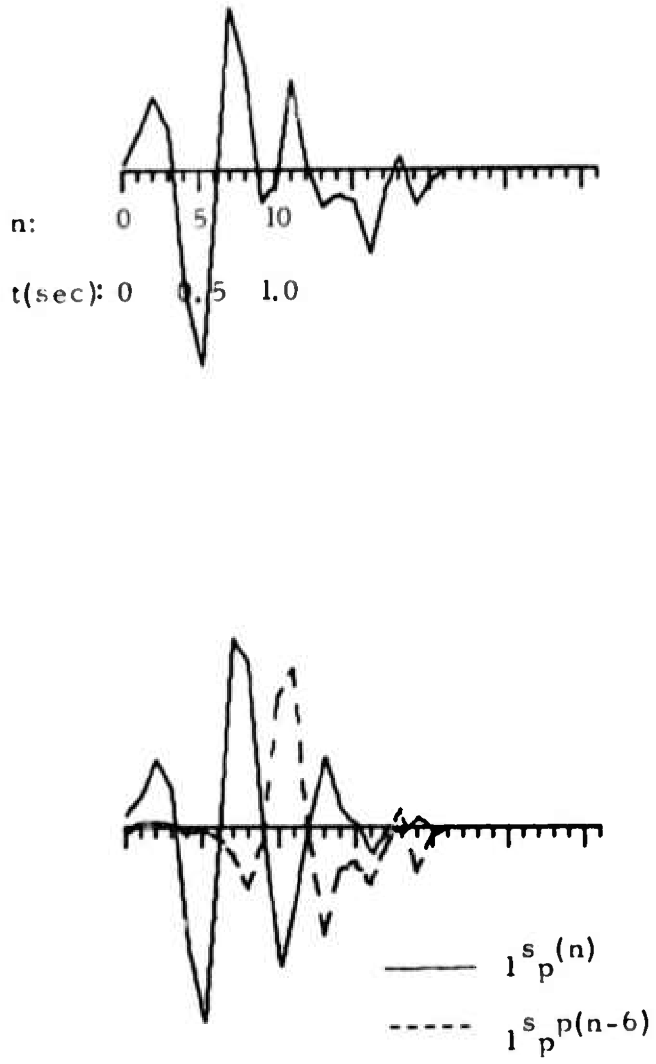

FIGURE III-1

WAVEFORMS OF SIGNAL, KA7/081/04N, AND CEPSTRUM RESOLVED SIGNALS $_1s_p(n)$ AND $_1s_pp(n-6)$

$$x_{SN}(n) = s_p(n) - as_p(n-n_o) + \alpha\epsilon(n) \qquad \text{(III-1)}$$

where $s_p(n)$ is the resolved P-phase from any one of the events listed in Table III-1, a and α are the scale constants, n_o is the delay time and $\epsilon(n)$ is the noise. In equation (III-1), $-s_p(n-n_o)$ simulates the surface reflection for the ideal case, where the surface reflected pP-phase is the exact replica of the P-phase. Thus, this synthetic mixed signal consists of two identical signals and some additive noise. Hence, the dissimilarity of the P-phase and the pP-phase does not enter into the problem and we can see the sole effect of the noise. The constant α is used to adjust the signal-to-noise ratio (SNR) such that we can examine the effect of various noise levels on the detection of the P-pP delay time and the successful decomposition of $x_{SN}(n)$. The typical waveforms and amplitude spectra of $x_{SN}(n)$ and $\epsilon(n)$ are given in Figure III-2 for SNR = ∞ and 24 dB.

To study the effect of the dissimilarity, the synthetic signals are formed as follows:

$$x_{SN}(n) = s_1(n) \pm s_2(n-n_o) \qquad \text{(III-2)}$$

where $s_1(n)$ is the resolved P-phase and $s_2(n)$ can be the resolved P-phase or pP-phase from any one of the events listed in Table III-1. The positive sign is used when the resolved pP-phase is assigned to $s_2(n)$ and the negative sign is for the resolved P-phase. Here $\pm s_2(n-n_o)$ simulates the imperfect surface reflection where the surface reflected pP-phase is not identical to the direct P-phase. The similarity coefficient of two time sequences, $x(n)$ and $y(n)$ is defined by (Harley, 1971)

$$\rho(x, y) = \frac{\phi_{xy}(0)}{\sqrt{\phi_{xx}(0)\,\phi_{yy}(0)}}$$

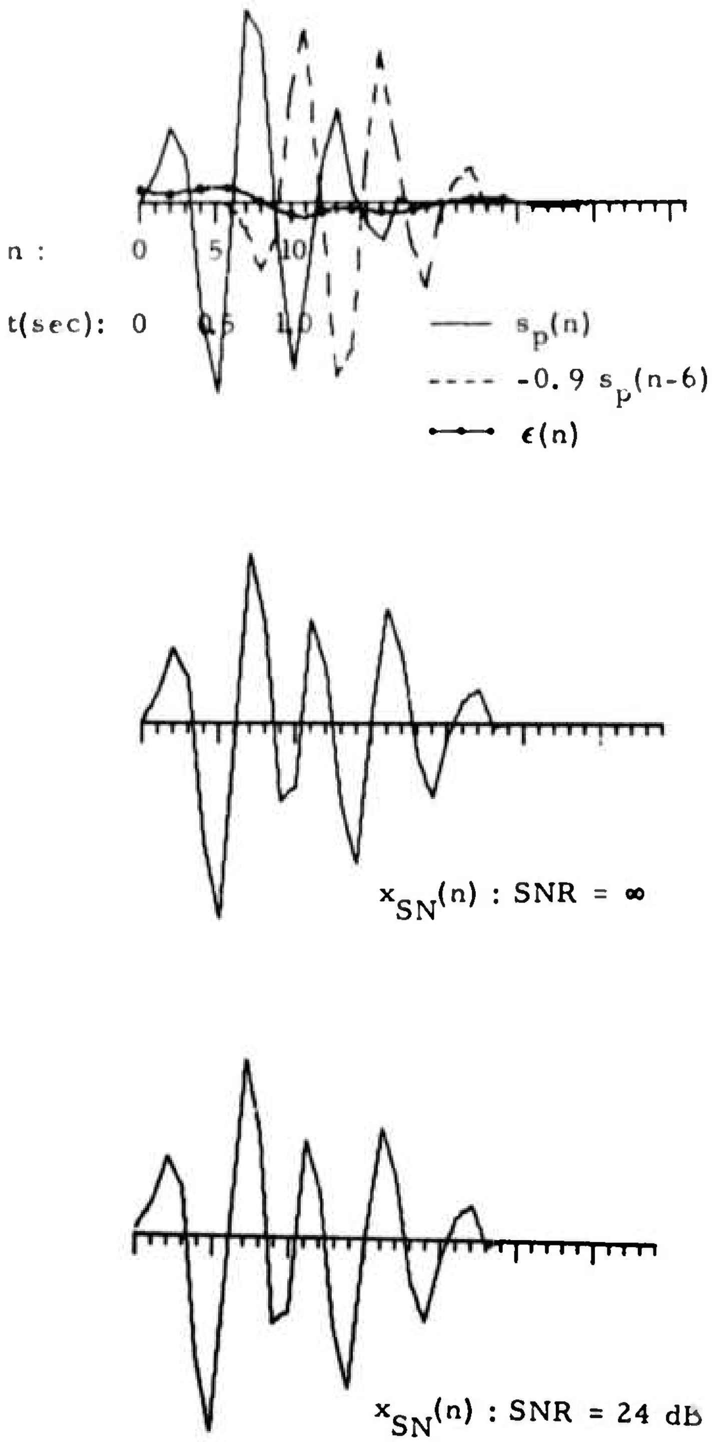

FIGURE III-2a

WAVEFORMS OF NOISE AND SYNTHETIC SIGNAL MADE FROM THE RESOLVED P-PHASE OF KAZ/081/04N

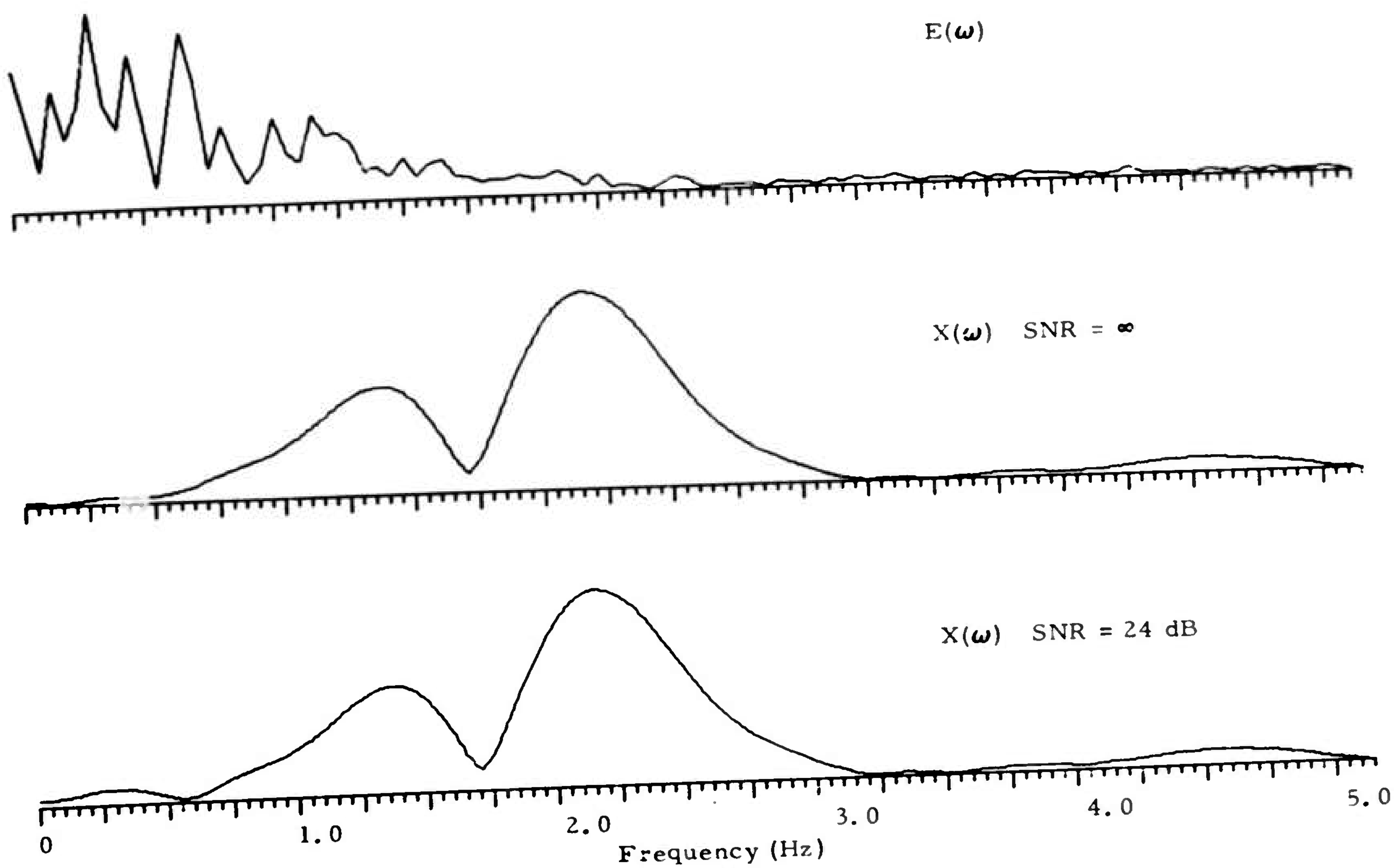

FIGURE III-2b

AMPLITUDE SPECTRA OF $\epsilon(n)$ AND $x_{SN}(n)$

where $\phi_{xy}(0)$ is the zero lag crosscorrelation value of $x(n)$ and $y(n)$, and $\phi_{xx}(0)$ and $\phi_{yy}(0)$ are the zero lag autocorrelation values of $x(n)$ and $y(n)$ respectively. The similarity coefficient of any two resolved phases is found to be in the range of 0.55 - 0.95 (see subsection C). Hence, we can show the effect of the dissimilarity on the cepstrum analyzed results by selecting $s_1(n)$ and $s_2(n)$ with varying similarity coefficients.

B. THE EFFECT OF NOISE

Four groups of noisy mixed signals were synthetically constructed from the resolved P-phases of four events listed in Table III-1 (according to the equation (III-1)). In each group there are thirty synthetic signals corresponding to six noise levels and five delay times (SNR = ∞, 30, 24, 18, 12, 6 dB and n_o = 4, 5, 6, 7, 8 sampling units). Here the signal-to-noise ratio is the ratio of RMS signal to RMS noise and one sampling unit corresponds to 0.1 second. The choice of the ranges for SNR and n_o is made to reflect the actual situation often encountered in the real EKAZ events, namely:

- The NORSAR recorded short-period P-waves of EKAZ events usually have SNR between 10 dB and 35 dB for m_b of 4.9 to 5.8.
- According to the cube root scaling law, the P-pP delay time for the contained explosion can range from 0.3 second to 0.8 second for m_b of 4.5 to 6.0 (Lane and Sun, 1974b).
- The shortest delay time that the complex cepstrum technique can resolve is about 0.4 second (Lane and Sun, 1974a, b).

The typical results are presented in Figure III-3 through Figure III-9 for the group of synthetic signals made from the resolved P-phase of the event KAZ/081/04N. That is, the synthetic signals are

$$x_{SNi}(n) = {}_1s_p(n) - a_1\, {}_1s_p(n-6) + \alpha_i \epsilon(n) \qquad i = 1, 2, \ldots, 6 \qquad \text{(III-3)}$$

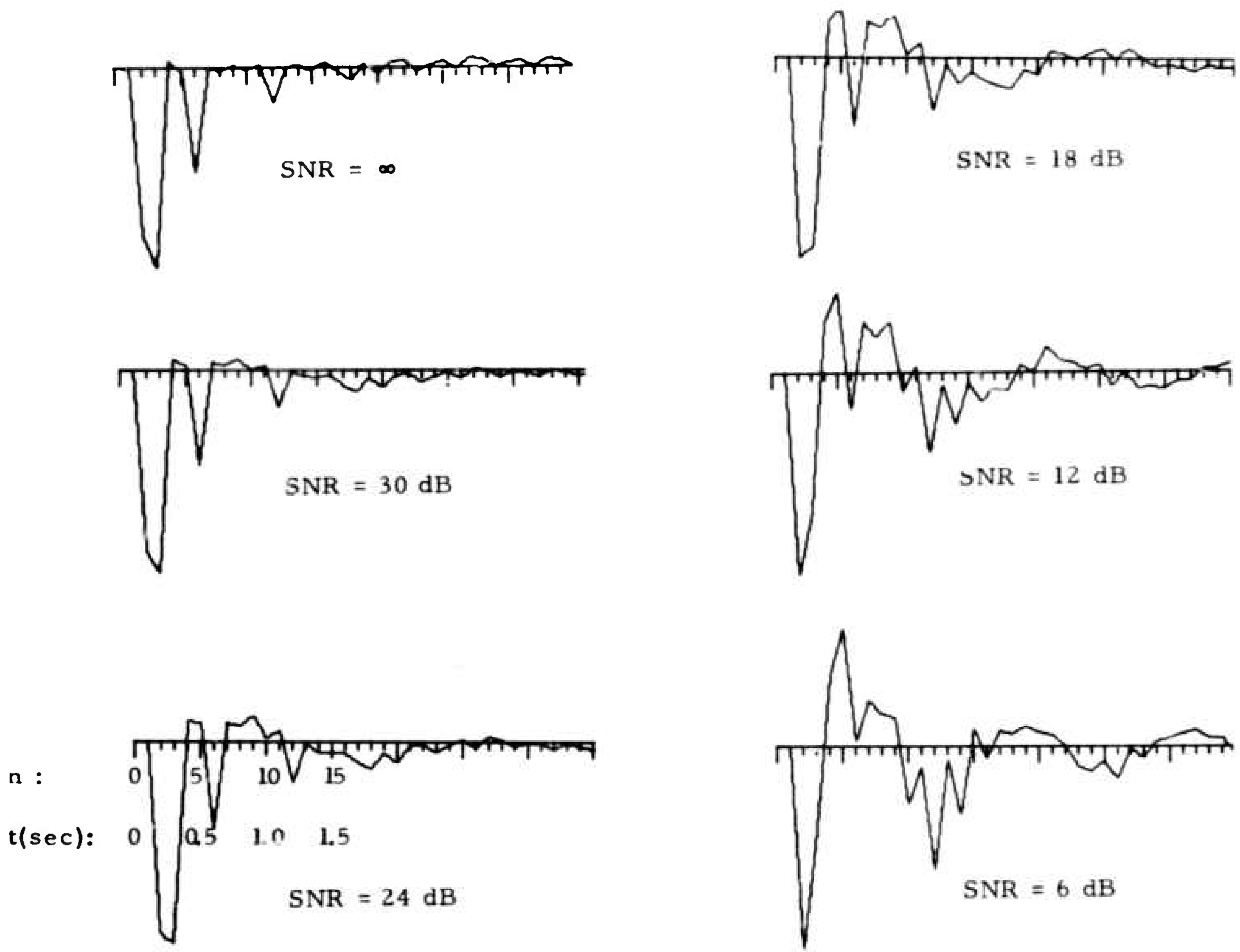

FIGURE III-3

CEPSTRA OF SYNTHETIC SIGNAL $x_{SN}(n)$ WITH VARYING SNR

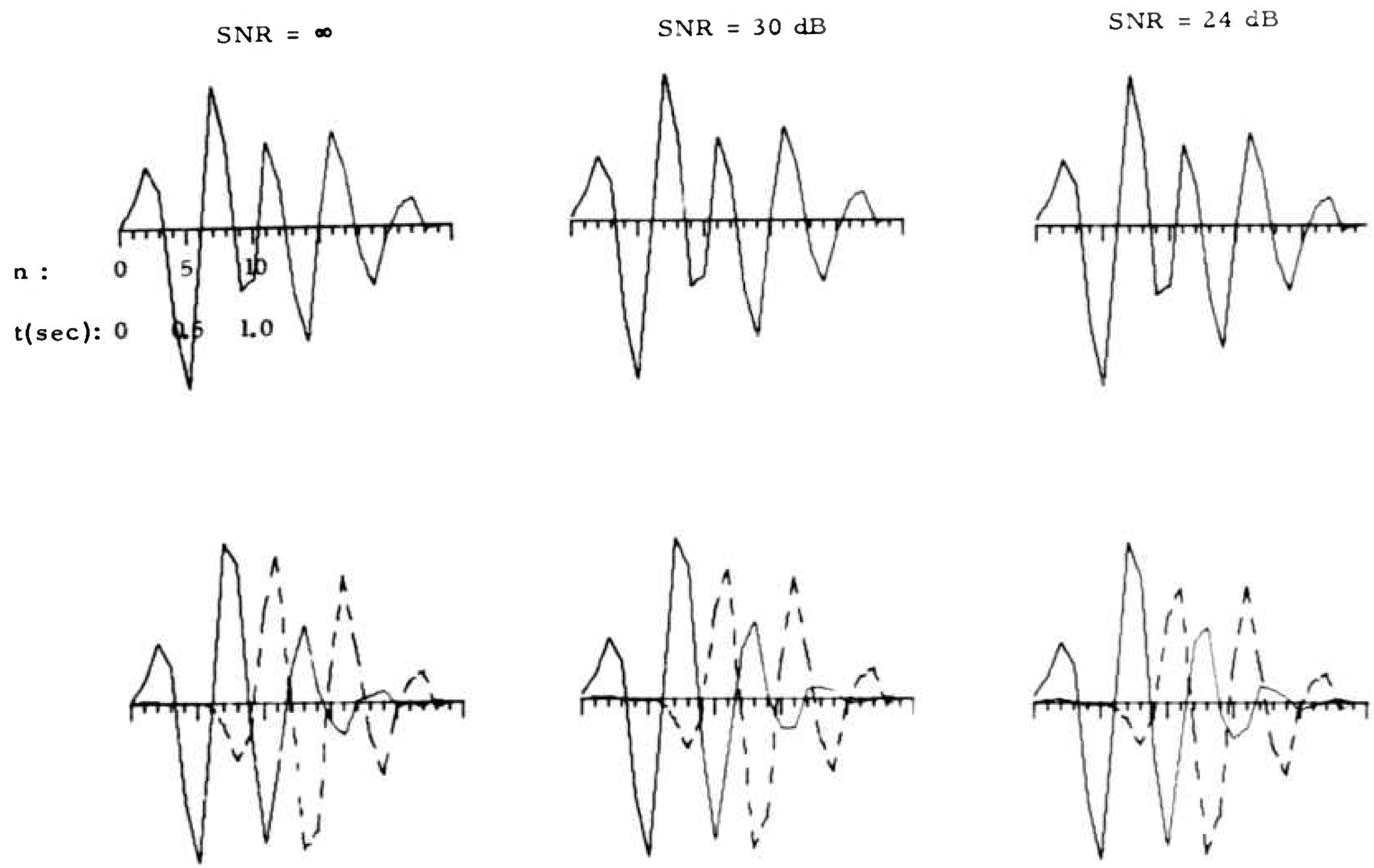

FIGURE III-4

WAVEFORMS OF SYNTHETIC SIGNALS, $x_{SNi}(n)$, AND CEPSTRUM RESOLVED SIGNALS, $\underset{\sim}{s}_p(n)$ AND $\underset{\sim}{s}_p P(n-\underset{\sim}{n}_{oi})$, WITH VARYING SNR

(PAGE 1 OF 2)

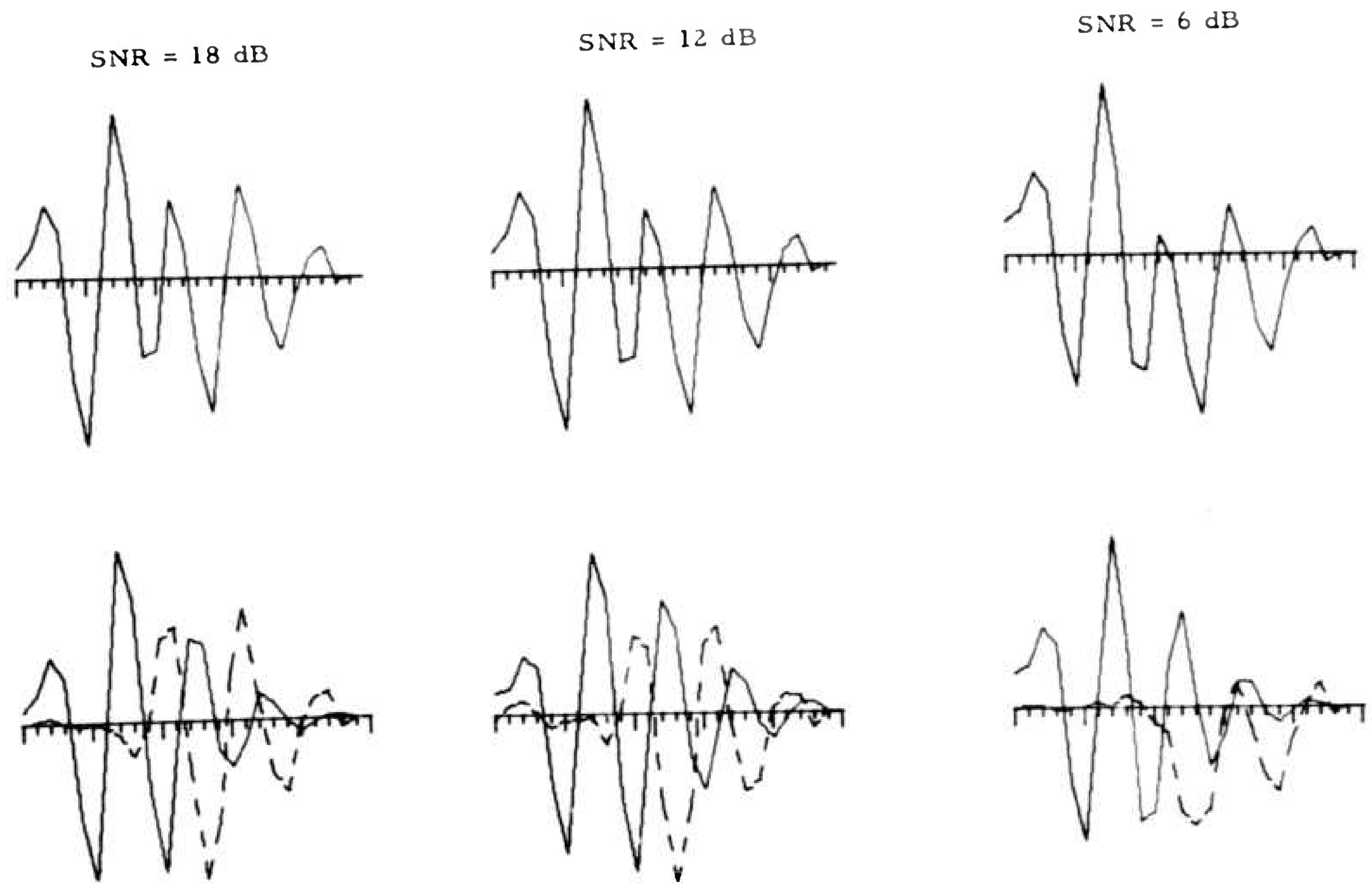

FIGURE III-4

WAVEFORMS OF SYNTHETIC SIGNALS, $x_{SNi}(n)$, AND CEPSTRUM RESOLVED SIGNALS, $\underset{\sim}{s}_p(n)$ AND $\underset{\sim}{s}_p P(n-\underset{\sim}{n}_{oi})$, WITH VARYING SNR
(PAGE 2 OF 2)

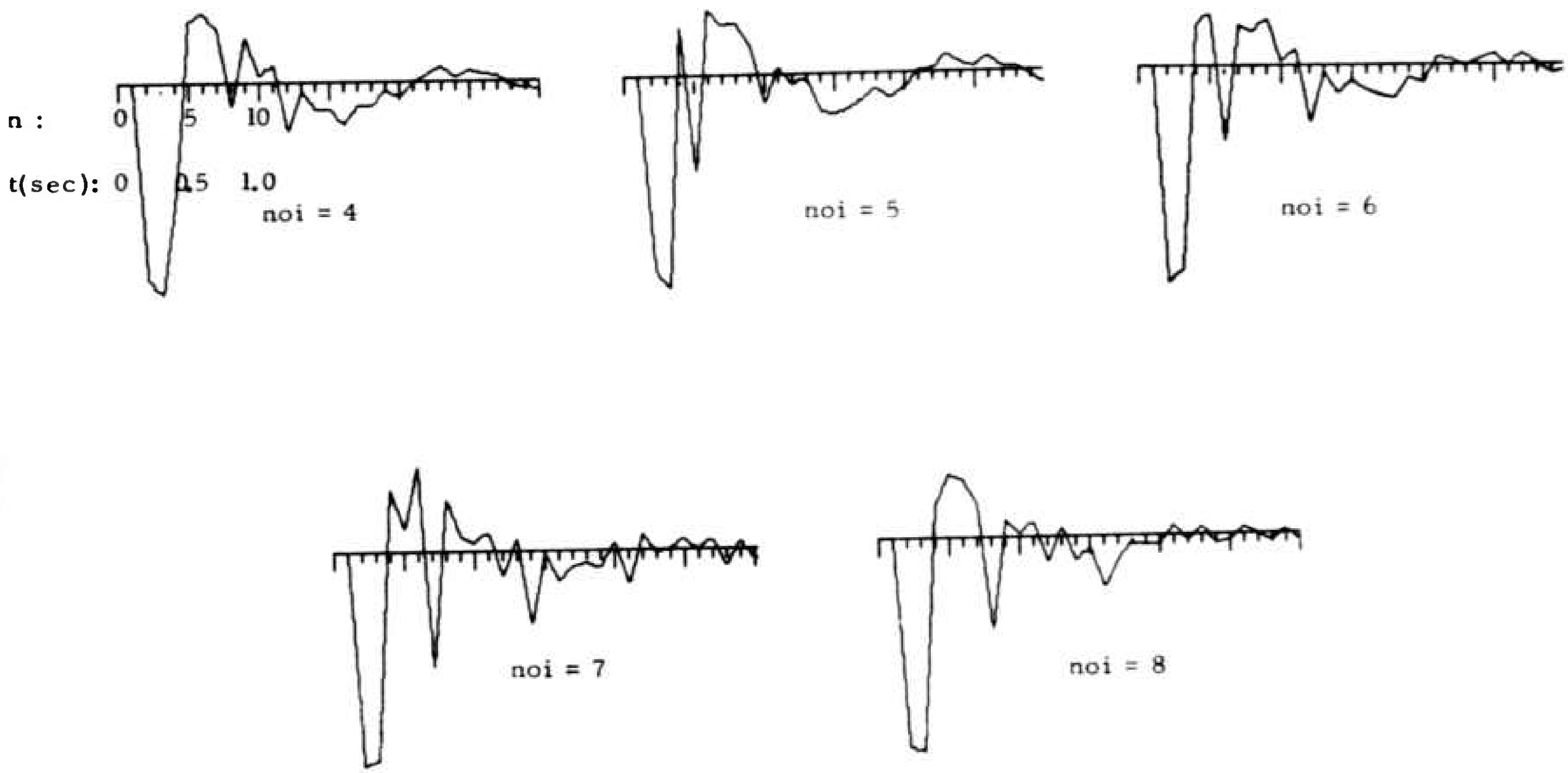

FIGURE III-5

CEPSTRA OF SYNTHETIC SIGNAL $x_{SNi}(n)$ WITH VARYING P-pP DELAY TIME, SNR = 18 dB

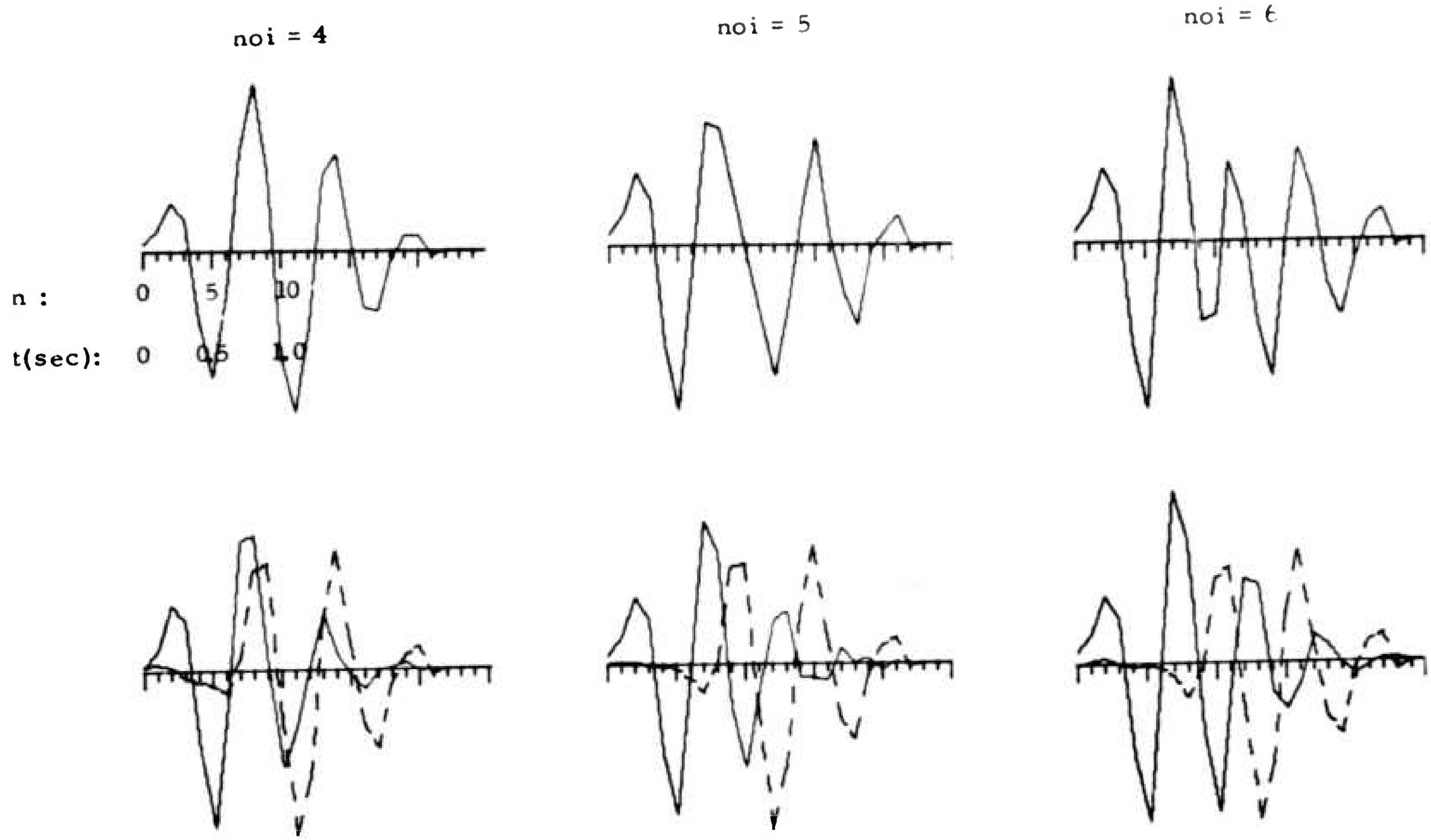

FIGURE III-6

WAVEFORMS OF SYNTHETIC SIGNALS, $x_{SNi}(n)$, AND CEPSTRUM RESOLVED SIGNALS, $\tilde{s}_p(n)$ AND $\tilde{s}_p(n-\ell_{oi})$, SNR = 18 dB

(PAGE 1 OF 2)

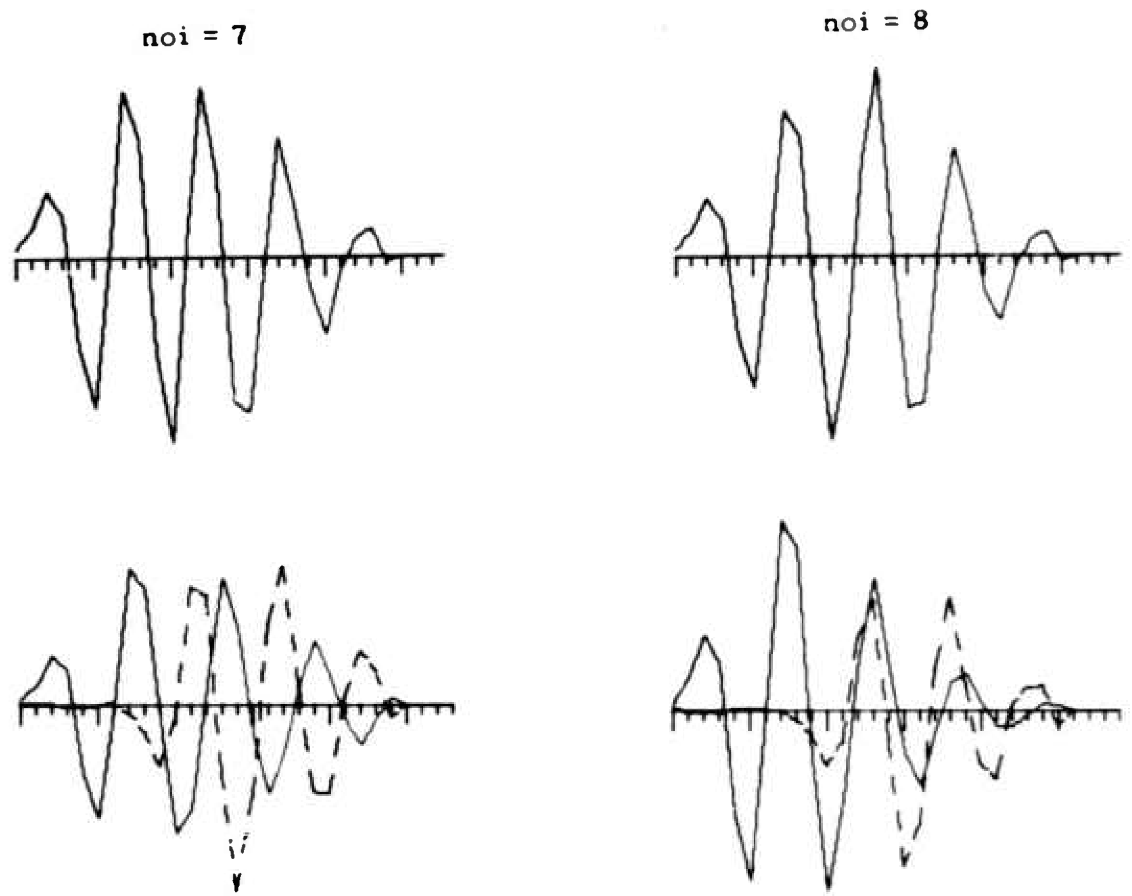

FIGURE III-6

WAVEFORMS OF SYNTHETIC SIGNALS, $x_{SNi}(n)$, AND CEPSTRUM RESOLVED SIGNALS, $\tilde{s}_p(n)$ AND $\tilde{s}_p(n-\tilde{n}_{oi})$, SNR = 18 dB

(PAGE 2 OF 2)

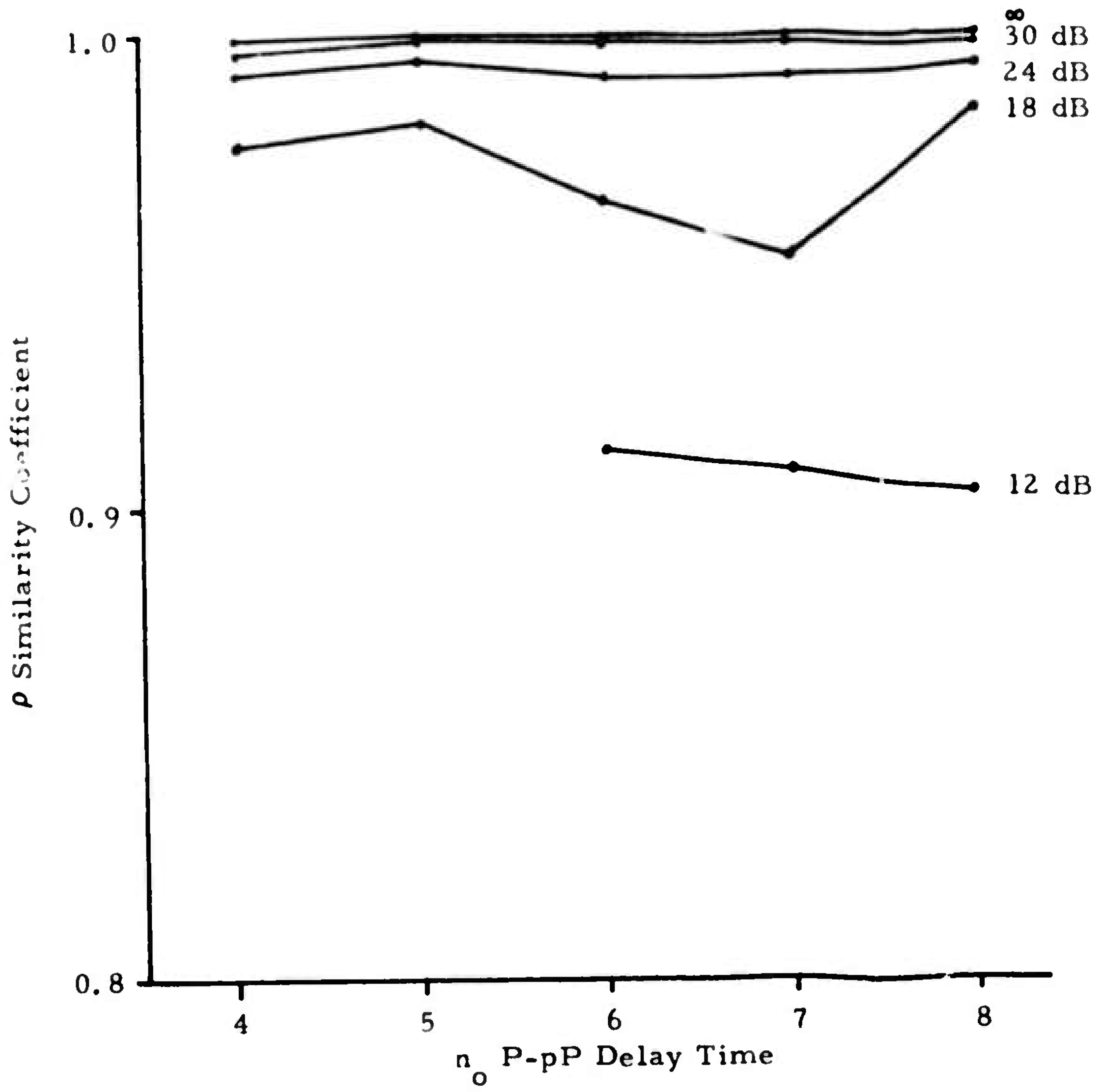

FIGURE III-7

SIMILARITY COEFFICIENTS OF $\hat{s}_p(n)$ AND $s_p(n)$

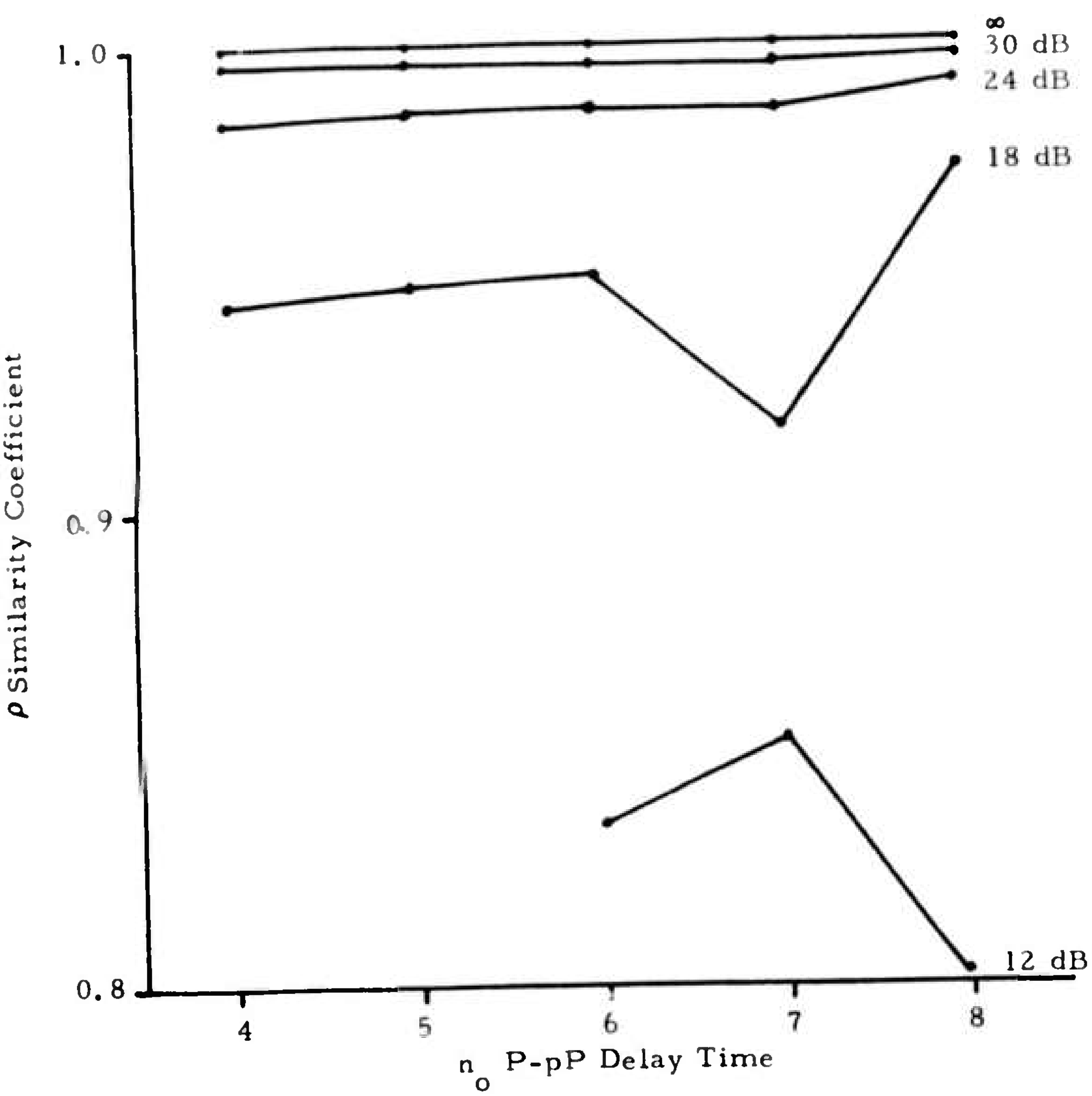

FIGURE III-8

SIMILARITY COEFFICIENTS OF $\underset{\sim}{s}_p P(n-\underset{\sim}{n}_{oi})$ AND $-s_p(n-n_{oi})$

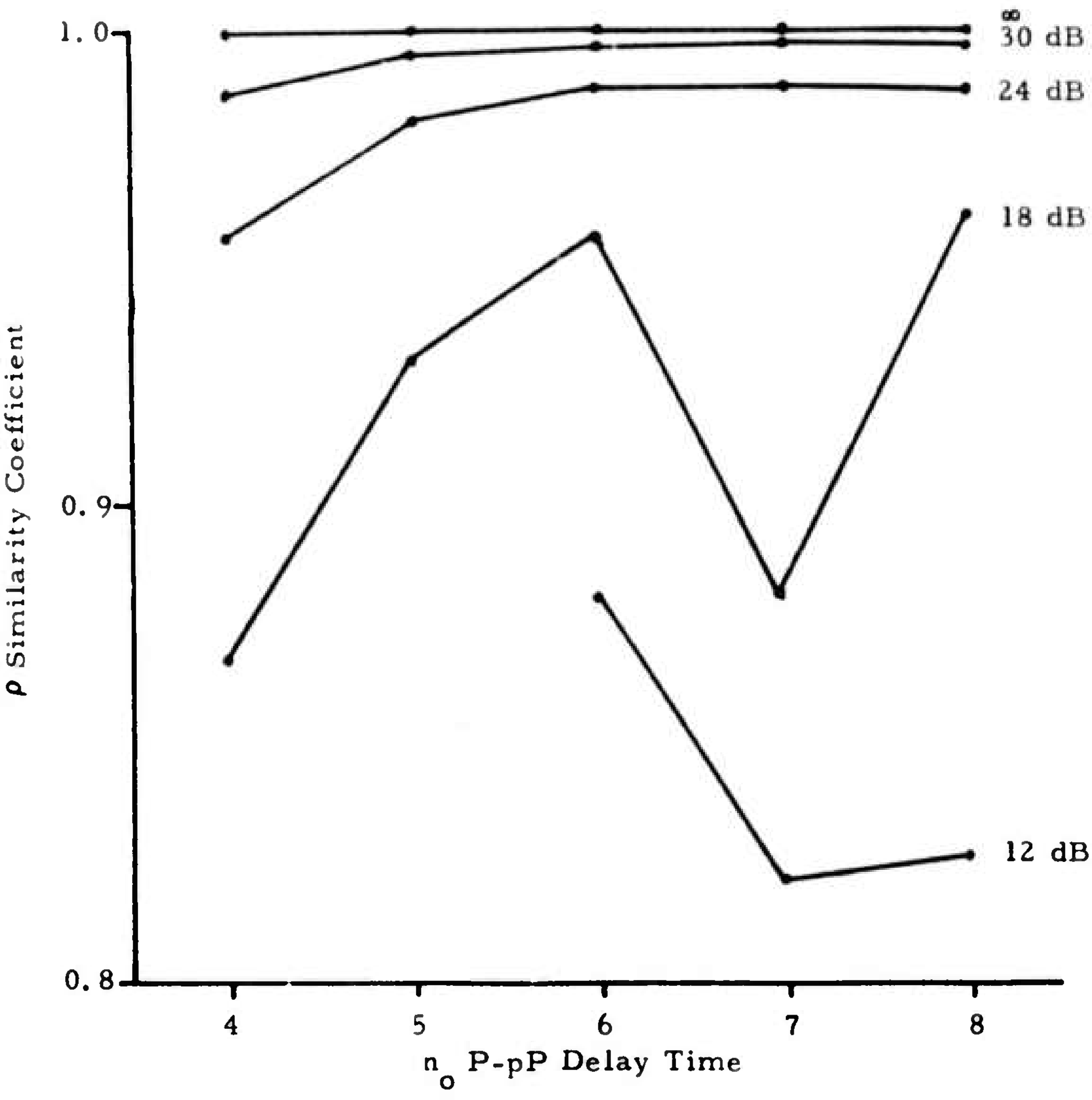

FIGURE III-9

SIMILARITY COEFFICIENTS OF $s_p(n)$ AND $s_p P(n-n_{oi})$

where α_i can assume six values corresponding to six levels of SNR and a is arbitrarily assigned to be 0.9 here.

Figure III-3 shows the cepstra of the signals with delay time $n_o = 6$ for six different values of SNR. This figure illustrates the effect of the noise on the detection of the P-pP delay time for the fixed delay time. In this figure, it is noticed that the cepstrak peaks due to the P-pP delay time do appear at $n = 6 \cdot k$, $k = 1, 2, 3$ as predicted in equation (II-5). How well these cepstral peaks can be distinguished from the surrounding cepstra obviously depends on the signal-to-noise ratio. When there is no noise (i.e., SNR = ∞), the cepstral peaks appear clearly at n = 6, 12, and 18. For SNR = 30 dB, the appearance of these cepstral peaks remains more or less the same as that for SNR = ∞, except that the surrounding cepstra start growing and interferring with the cepstral peak at n = 18. The magnitudes of the surrounding cepstra keep increasing and the interference becomes more serious as the signal-to-noise ratio decreases. Nevertheless, the first two cepstral peaks can still be distinguished quite well for SNR = 24 and 18 dB. For SNR = 12 and 6 dB, these cepstral peaks are buried in the surrounding cepstra in the sense that they can not be easily recognized as in the higher SNR cases. Thus, strictly speaking, for SNR = 12 dB, it should be concluded that the cepstral peaks due to the P-pP delay time cannot be detected. However, in most cases analyzed here, we can detect these cepstral peaks by carefully examining the relative positions of all suspicious cepstral peaks and looking for the periodicity which should exist for them due to the P-pP delay time as described by the second term in equation (II-5).

Applying the shortpass filter to the cepstra shown in Figure III-3 at n = 6, the cepstrum analysis decomposes $x_{SNi}(n)$ into the following form

$$x_{SNi}(n) = \underset{\sim}{s}_p(n) + \underset{\sim}{s}_p P(n - \underset{\sim}{n}_{oi}) , \tag{III-4}$$

where $\tilde{s}_p(n)$ and $\tilde{s}_p P(n - \tilde{n}_{oi})$ are the cepstrum resolved signals which are expected to be the estimates of $s_p(n)$ and $-s_p(n-6)$, respectively. Figure III-4 shows the waveforms of $x_{SNi}(n)$ and the cepstrum resolved signals. In this figure, $\tilde{s}_p(n)$ is in the solid line and $\tilde{s}_p P(n - \tilde{n}_{oi})$ is in the dashed line. It can be seen that the waveform of $x_{SNi}(n)$ remains very much the same for SNR down to 18 dB. For SNR = ∞, 30, 24, and 18 dB, the separation of $\tilde{s}_p(n)$ and $\tilde{s}_p P(n - \tilde{n}_{oi})$ is clean and the estimate of the delay time $\tilde{n}_{oi}$ is 6, which is the actual delay time between s_p and $-s_p(n-6)$. For SNR = 12 dB, although the separation is not clean, the estimate of the delay time is still 6. For SNR = 6 dB, it is clear that the cepstrum analysis fails to decompose $x_{SNi}(n)$ properly. By comparing equations (III-3) and (III-4), it can be seen that the noise in $x_{SNi}(n)$ is somehow distributed between $\tilde{s}_p(n)$ and $\tilde{s}_p P(n - \tilde{n}_{oi})$. However, the good resemblance of $\tilde{s}_p(n)$ and $s_p(n)$ (solid line in Figure III-2) and that of $\tilde{s}_p P(n - \tilde{n}_{oi})$ and $-s_p(n-6)$ (dashed line in Figure III-2) are clearly observed. This indeed is quantitatively reflected in the appropriate similarity coefficients given in Table III-2. All similarity coefficients are well above 0.9, except those for SNR = 12 dB. For SNR = 12 dB, they are still well above 0.8 which in general is considered quite similar. It is noticed that the similarity between $\tilde{s}_p(n)$ and $s_p(n)$ is better than that between $\tilde{s}_p P(n - \tilde{n}_{oi})$ and $-s_p(n-6)$. This might imply that the noise is not equally divided between the resolved signals. The second resolved signal $\tilde{s}_p P$ is noiser.

Figure III-5 shows the complex cepstra of the signals with SNR = 18 dB for five different delay times. That is, the synthetic signals are

$$x_{SNi}(n) = s_p(n) - s_p(n - n_{oi}) + \alpha\epsilon(n) \qquad \text{(III-5)}$$

where n_{oi} = 4, 5, 6, 7, and 8. This figure shows the effect of varying delay time on the detection of the P-pP delay time for the fixed noise level. There

TABLE III-2

SIMILARITY COEFFICIENTS FOR VARIOUS SNR AND P-pP DELAY TIME OF 0.6 SECONDS

SNR (dB)	$\rho(\underset{\sim}{s}_p, s_p)$	$\rho(\underset{\sim}{s}_p P, -s_p)$	$\rho(\underset{\sim}{s}_p, -\underset{\sim}{s}_p P)$
∞	1.0	1.0	1.0
30	0.997	0.996	0.997
24	0.989	0.986	0.988
18	0.915	0.950	0.956
12	0.912	0.834	0.881
6	-	-	-

$\rho(x, y)$: similarity coefficient of signals $x(n)$ and $y(n)$

is a weak indication that the detection of the cepstral peaks due to the P-pP delay time is better for large n_{oi}. Nevertheless, these cepstral peaks can be identified without difficulty for n_{oi} down to 5 and they all appear at the correct cepstrum times, i.e., $n = kn_{oi}$, $k = 1, 2, \ldots$ as indicated by the equation (II-5). For $n_{oi} = 4$, the cepstral peak at $n = 4$ is concealed by the cepstrum of the signal $s_p(n)$. Hov ever, those at $n = 8$ and 12 can still be identified with careful examination as previously mentioned. Figure III-6 gives the waveforms of $x_{SNi}(n)$ and the cepstrum resolved signals. Again, the resolved signals closely resemble the original signals. The similarity coefficients, given in Table III-3, are all well above 0.9. There is no definite relation between the similarity coefficient and the delay time. In other words, the longer delay time does not necessarily imply better or worse similarity, one way or the other. However, the similarity between $\underset{\sim}{s}_p(n)$ and $s_p(n)$ is better than that between $\underset{\sim}{s}_p P(n - \underset{\sim}{n}_{oi})$ and $-s_p(n - n_{oi})$ as was found for the case of fixed delay time and varying SNR.

In Figures III-7 through III-9, the similarity coefficient of $\underset{\sim}{s}_p(n)$ and $s_p(n)$, that of $\underset{\sim}{s}_p P(n - \underset{\sim}{n}_{oi})$ and $-s_p(n - n_{oi})$, and that of $\underset{\sim}{s}_p(n)$ and $\underset{\sim}{s}_p P(n - \underset{\sim}{n}_{oi})$ are plotted as functions of the P-pP delay time n_{oi} using signal-to-noise ratio as the parameter. These figures display clearly the relation amont the similarity coefficient, the P-pP delay time, and the signal-to-noise ratio.

The major results from the study on the effect of the noise are as follows:

- The cepstral peaks due to the P-pP delay time can be identified for signal-to-noise ratio down to 12 dB and the P-pP delay time as short as 0.4 seconds.
- The cepstrum analysis can successfully recover the P-phase and pP-phase for the P-pP delay time down to 0.4 seconds with

TABLE III-3

SIMILARITY COEFFICIENTS FOR VARIOUS P-pP DELAY TIMES AND SNR OF 18 dB

P-pP Delay Time (Seconds)	$\rho(\underset{\sim}{s}_p , s_p)$	$\rho(\underset{\sim}{s}_p P , -s_p)$	$\rho(\underset{\sim}{s}_p , -\underset{\sim}{s}_p P)$
0.8	0.984	0.975	0.962
0.7	0.914	0.917	0.879
0.6	0.965	0.950	0.956
0.5	0.982	0.949	0.931
0.4	0.977	0.945	0.867

$\rho(x, y)$: similarity coefficient of signals $x(n)$ and $y(n)$

signal-to-noise ratio above 18 dB and to 0.6 seconds with SNR = 12 dB.

- For the fixed P-pP delay time, the detection of the cepstral peaks is clearly better for high signal-to-noise ratio. The similarity coefficients increase significantly with the increasing signal-to-noise ratio.
- For the fixed noise level, there is only a weak indication that the detection of the cepstral peaks is better for large P-pP delay time. For high signal-to-noise ratio (SNR > 18 dB), the similarity coefficients increase slightly as the P-pP delay time increases. However, there is no such relation observed for SNR $\leq$ 12 dB.
- The similarity coefficient of $\underset{\sim}{s}_p$ and s_p is higher than that of $\underset{\sim}{s}{}_p^{P}$ and $-s_p$. This implies that the noise will seriously affect the recovery of the pP-phase.

C. THE EFFECT OF DISSIMILARITY

From the eight cepstrum resolved phases of the EKAZ events listed in Table III-1, eight synthetic signals are made according to equation (III-2) for the delay time of 0.6 second (i.e., $n_o = 6$). To facilitate the discussion below, a nomenclature is established for these synthetic signals in Table III-4. Also given in this table are the similarity coefficients of $s_1(n)$ and $s_2(n)$. It is noticed that these similarity coefficients vary from 0.55 to 1.0. Thus, the analysis of these synthetic signals simulates the situation where the mixed signal consists of two non-identical signals with varying degree of similarity.

The cepstra of $x_{SD}(n)$ are shown in Figure III-10. For the signal SMD-I which consists of two identical signals, the cepstral peaks due

TABLE III-4

SYNTHETIC SIGNAL CONSISTING OF TWO NON-IDENTICAL SIGNALS WITH VARYING DEGREE OF SIMILARITY

Signal I. D. $X_{SD}(n)$*	$s_1(n)$	$s_2(n)$	$\rho(s_1, s_2)$
SMD-1	${}_1s_p(n)$	$-{}_1s_p(n)$	1.0
SMD-2	${}_1s_p(n)$	${}_3s_pP(n)$	0.933
SMD-3	${}_1s_p(n)$	${}_2s_pP(n)$	0.856
SMD-4	${}_1s_p(n)$	$-{}_3s_p(n)$	0.844
SMD-5	${}_1s_p(n)$	$-{}_4s_p(n)$	0.798
SMD-6	${}_1s_p(n)$	${}_1s_pP(n)$	0.712
SMD-7	${}_1s_p(n)$	$-{}_2s_p(n)$	0.699
SMD-8	${}_1s_p(n)$	${}_4s_pP(n)$	0.559

* $X_{SD}(n) = s_1(n) + s_2(n-6)$

$\rho(s_1, s_2)$: similarity coefficient of $s_1(n)$ and $s_2(n)$

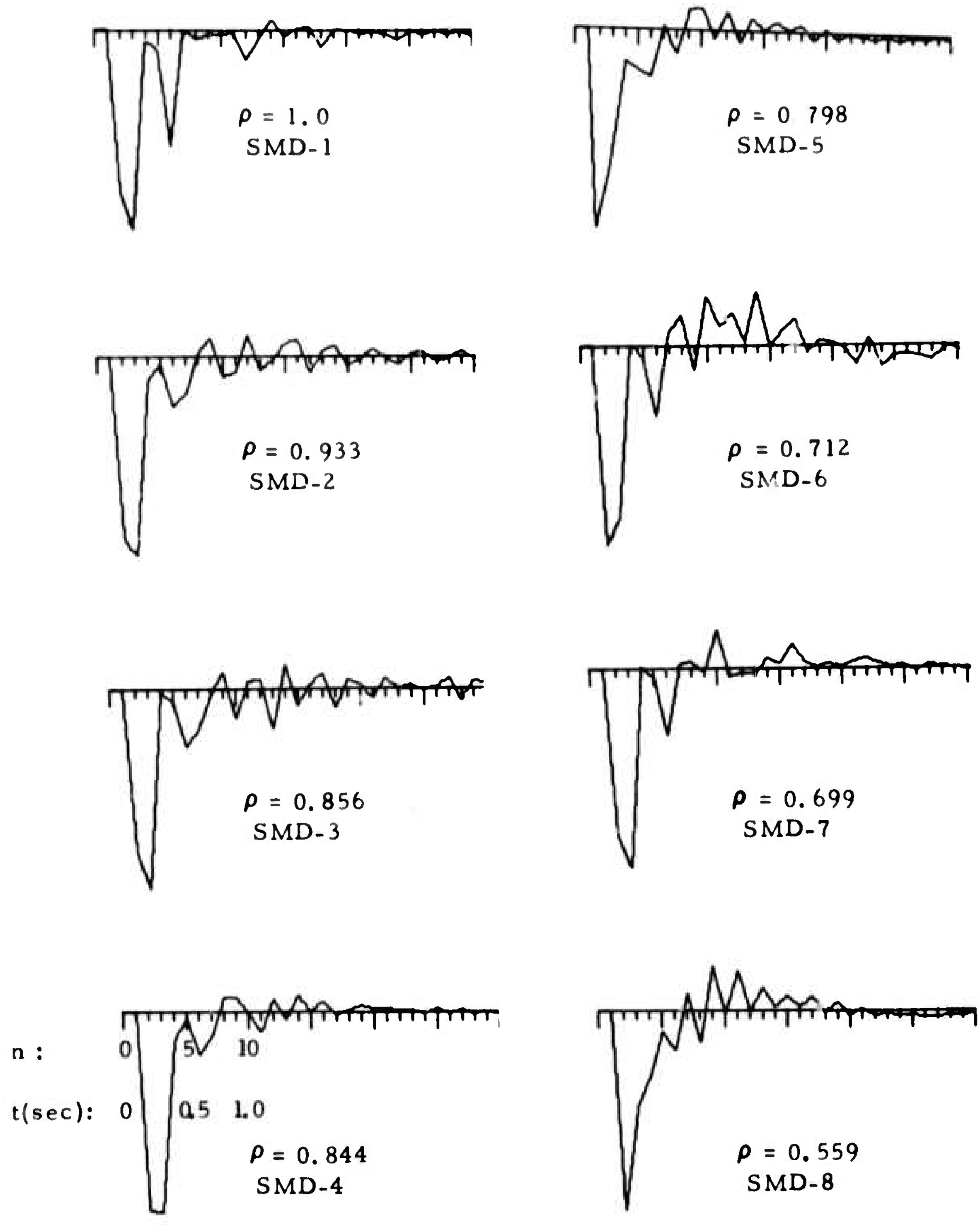

FIGURE III-10

CEPSTRA OF SYNTHETIC SIGNALS, $x_{SD}(n)$, FOR VARYING SIMILARITY BETWEEN $s_1(n)$ AND $s_2(n)$

to the P-pP delay time appear precisely at $n = 6k$, $k = 1, 2, 3, \ldots$, as predicted in equation (II-10) when $s_1(n)$ and $s_2(n)$ are identical. However, as soon as that $s_1(n)$ and $s_2(n)$ become non-identical, even for the signal SMD-2 with a high similarity of 0.933, the nice periodic occurrance of these cepstral peaks disappears. Thus, in general, the cepstral peaks due to the P-pP delay time do not exhibit the periodicity as predicted by the second term in the equation (II-10). Nevertheless, a cepstral peak, although not as sharp as theoretically expected, is observed at $n=6$ where the first cepstral peak should appear. For a similarity coefficient greater than 0.7, the identification of this cepstral peak does not become more difficult as the similarity coefficient decreases.

Applying the shortpass filter to the cepstra at $n=6$, the cepstrum analysis decomposes these synthetic signals into the following form

$$x_{SD}(n) = \underset{\sim}{s}_1(n) + \underset{\sim}{s}_2(n-6) \qquad \text{for SMD-i, i = 1,8} \qquad \text{(III-6)}$$

The waveforms of these signals are given in Figure III-11. It can be seen that the resemblance between $\underset{\sim}{s}_1(n)$ and $s_1(n)$, and that between $\underset{\sim}{s}_2(n)$ and $s_2(n)$ are good. This is clearly shown by their similarity coefficients given in Table III-5. By comparing the positions of their corresponding amplitude peaks, the delay time between $\underset{\sim}{s}_1(n)$ and $\underset{\sim}{s}_2(n)$ is estimated to be 0.6 seconds as indicated in equation (III-6). This is exactly equal to that between $s_1(n)$ and $s_2(n)$. Therefore, cepstrum analysis successfully decomposes $x_{SD}(n)$ into its constituent parts.

The major results from the study on the effect of dissimilarity can be summarized as follows:

- The dissimilarity between $s_1(n)$ and $s_2(n)$ will destroy the periodicity of the cepstral peaks due to the P-pP delay time. However, the first cepstral peak does occur at the right cepstrum time which is equal to the P-pP delay time.

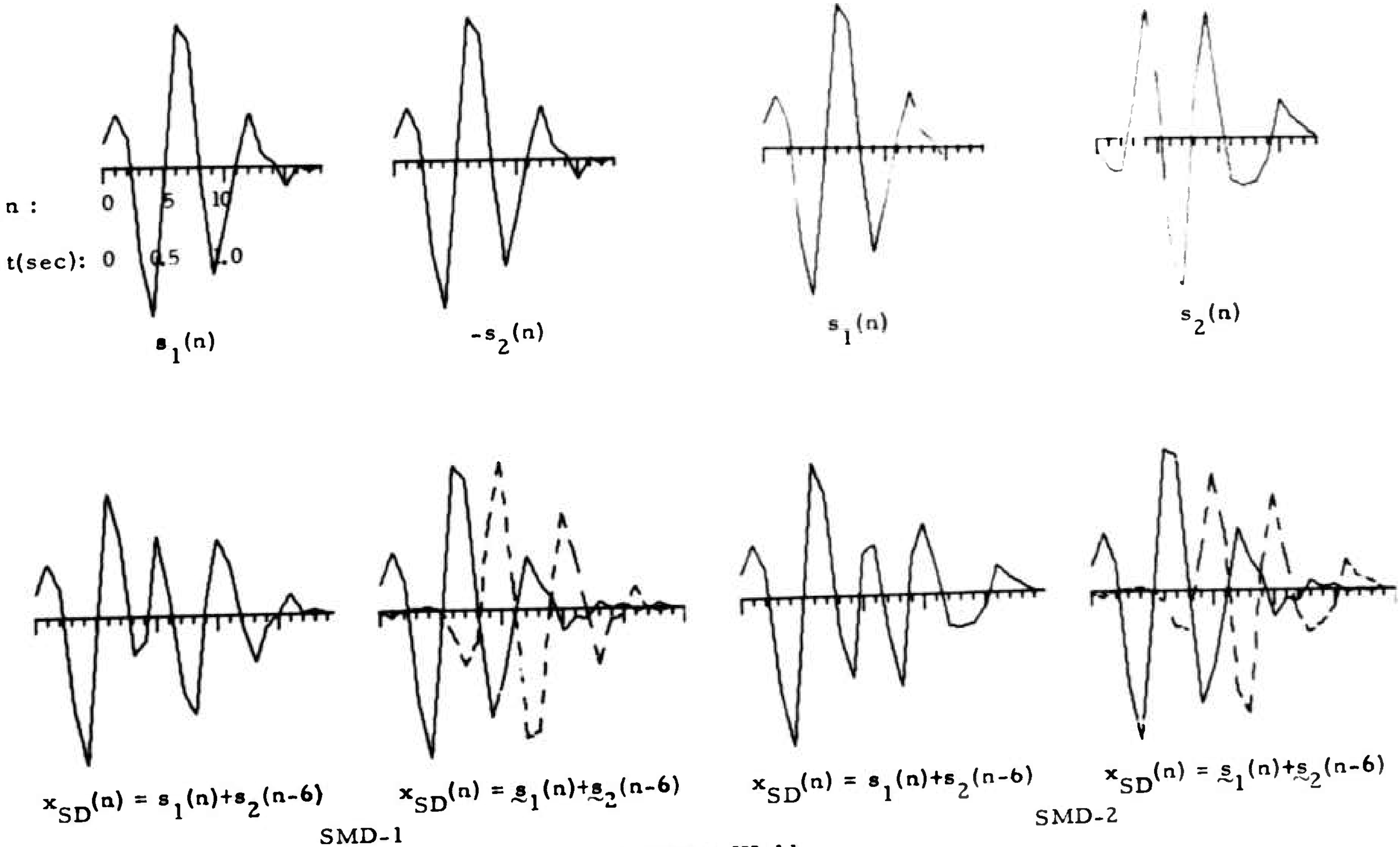

FIGURE III-11

WAVEFORMS OF SYNTHETIC SIGNALS, $x_{SD}(n)$, AND CEPSTRUM RESOLVED SIGNALS, $\tilde{s}_1(n)$ AND $\tilde{s}_2(n-6)$

(PAGE 1 OF 4)

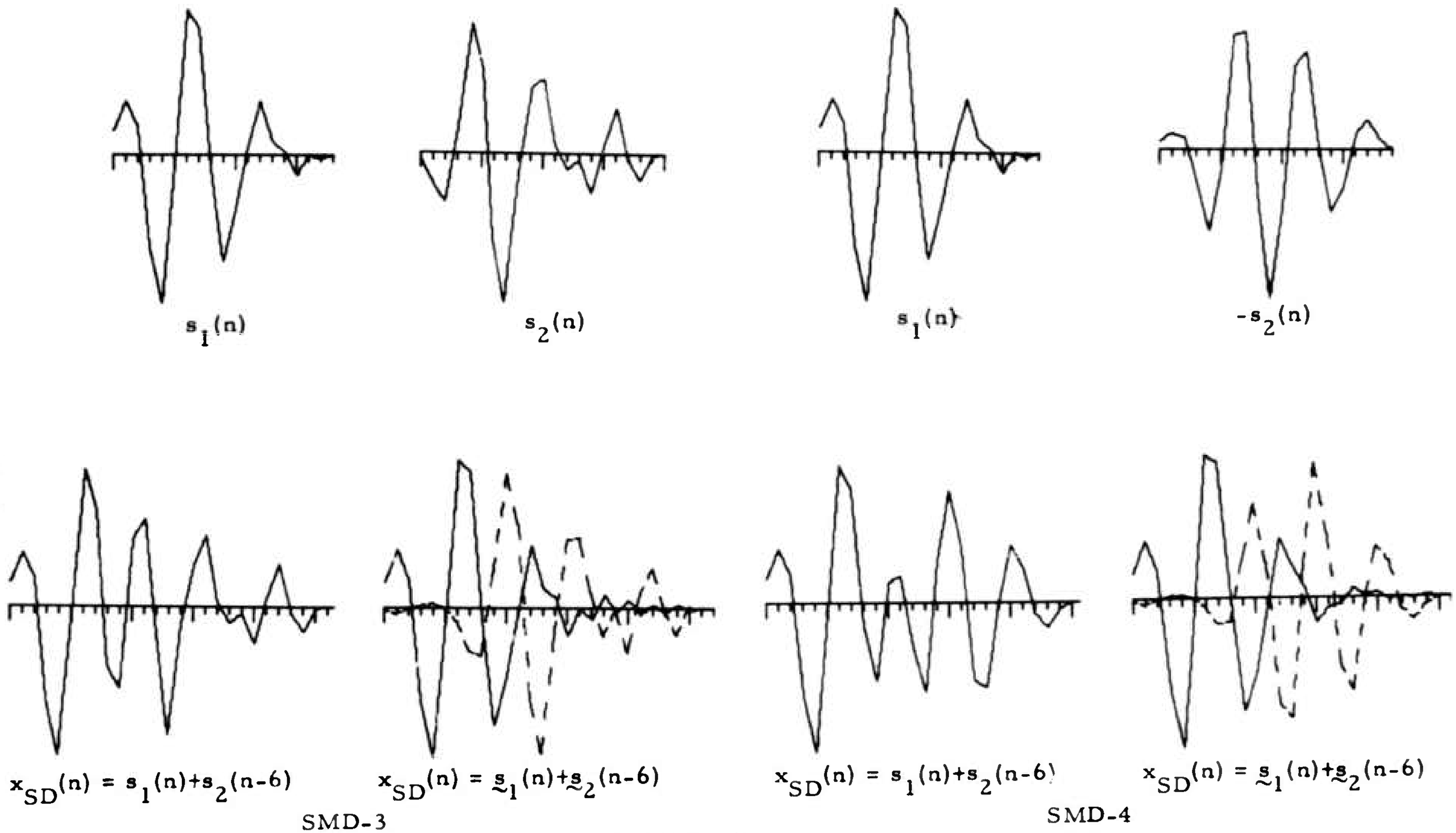

FIGURE III-11

WAVEFORMS OF SYNTHETIC SIGNALS, $x_{SD}(n)$, AND CEPSTRUM RESOLVED SIGNALS, $\underset{\sim}{s}_1(n)$ AND $\underset{\sim}{s}_2(n-6)$

(PAGE 2 OF 4)

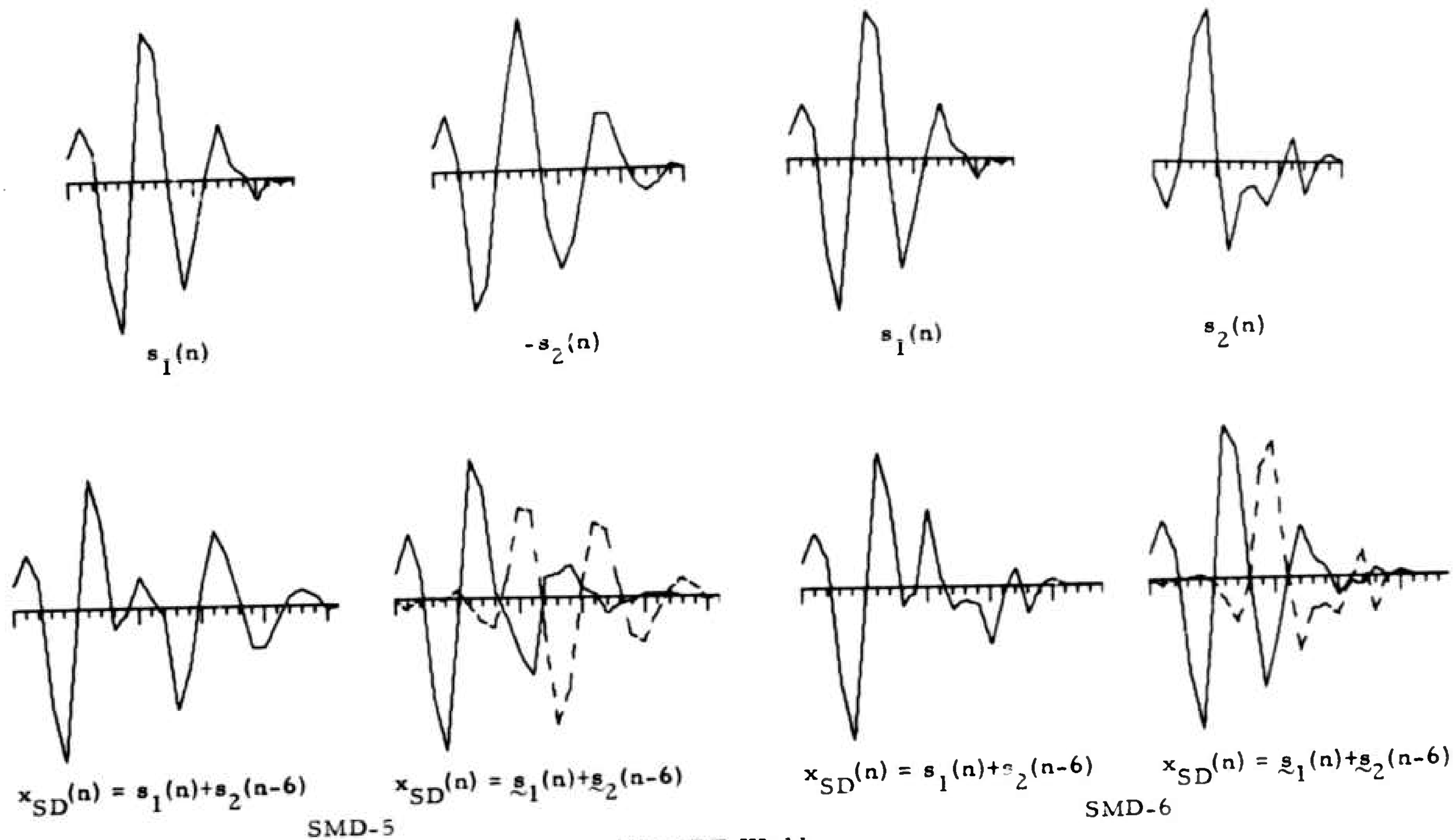

FIGURE III-11

WAVEFORMS OF SYNTHETIC SIGNALS, $x_{SD}(n)$, AND CEPSTRUM RESOLVED SIGNALS, $\underset{\sim}{s}_1(n)$ AND $\underset{\sim}{s}_2(n-6)$

(PAGE 3 OF 4)

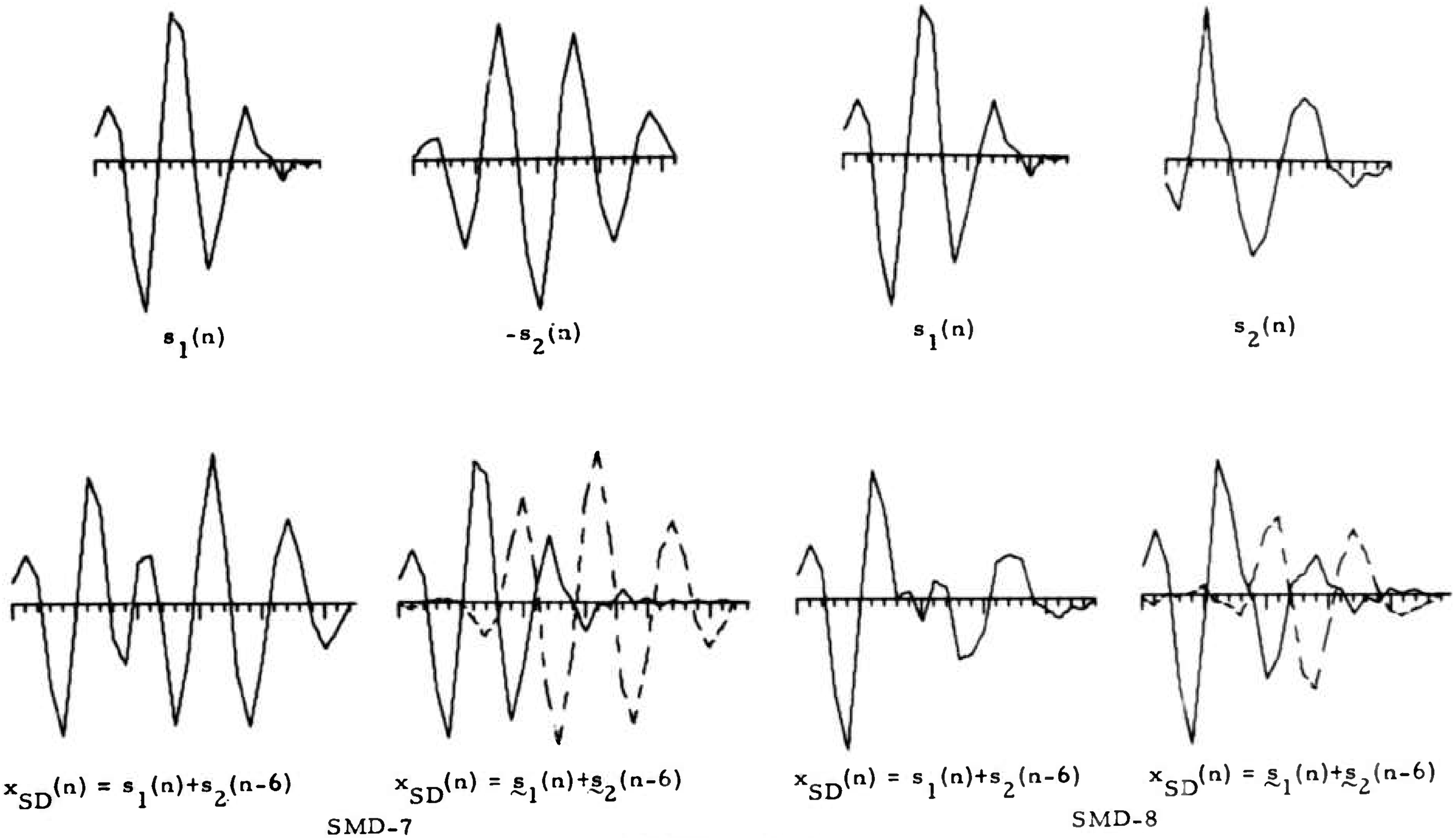

FIGURE III-11

WAVEFORMS OF SYNTHETIC SIGNALS, $x_{SD}(n)$, AND CEPSTRUM RESOLVED SIGNALS, $\tilde{s}_1(n)$ AND $\tilde{s}_2(n-6)$

(PAGE 4 OF 4)

TABLE III-5

SIMILARITY COEFFICIENTS FOR VARYING SIMILARITY BETWEEN $s_1(n)$ AND $s_2(n)$

Signal I. D.	$\rho(s_1, s_2)$	$\rho(\underset{\sim}{s}_1, \underset{\sim}{s}_2)$	$\rho(\underset{\sim}{s}_1, s_1)$	$\rho(\underset{\sim}{s}_2, s_2)$
SMD-1	1.0	1.0	1.0	1.0
SMD-2	0.933	0.938	0.991	0.991
SMD-3	0.856	0.884	0.997	0.995
SMD-4	0.844	0.870	0.992	0.992
SMD-5	0.798	0.781	0.995	0.998
SMD-6	0.712	0.723	0.918	0.890
SMD-7	0.699	0.735	0.891	0.826
SMD-8	0.559	0.564	0.871	0.833

$\rho(x, y)$: similarity coefficient of $x(n)$ and $y(n)$

- The identification of the first cepstral peak is independent of the similarity between $s_1(n)$ and $s_2(n)$. There is only a very weak indication that lower similarity may result in poor identification.
- The cepstrum resolved signals, $\underset{\sim}{s}_1(n)$ and $\underset{\sim}{s}_2(n)$, agree very well with the original signals, $s_1(n)$ and $s_2(n)$. Their similarity coefficients are well above 0.8.
- The identification of the first cepstral peak and the successful decomposition of $x_{SD}(n)$ by applying the shortpass filter at the occurrance of this cepstral peak will constitute the detection of the P-pP delay time. In this sense, cepstrum analysis can detect the P-pP delay time and successfully decompose $x_{SD}(n)$ for a similarity coefficient of $s_1(n)$ and $s_2(n)$ as low as 0.55.

By comparison of the results obtained here and those in the Subsection III-B, it is reasonable to say that the dissimilarity will affect the detection of the cepstral peaks due to the P-pP delay time more seriously than does the noise. In general, for a mixed signal consisting of two non-identical signals, we should not expect to find the periodicity of the cepstral peaks due to the P-pP delay time. Rather, we should look for the suspicious cepstral peaks and apply the shortpass filters accordingly. The correct estimate of the P-pP delay time can only be obtained through the successful cepstrum decomposition of the mixed signal $x_{SD}(n)$.

D. THE EFFECT OF PREFILTERING

It has been shown in Subsection B that, to some degree, the noise affects the detection of the cepstral peaks due to the P-pP delay time. The purpose of this experiment is to find out if the reduction of the noise by filtering before cepstrum analysis will improve detection. The experiment is carried out on the same synthetic signals as those used in Subsection B. From the amplitude spectra of the noise and the synthetic signal (SNR = ∞) shown in Figure III-2a, it is noticed that the noise spectrum is confined below 2.5 Hz and the signal has significant spectral content from 0.5 Hz to the folding frequency which is 5 Hz. Thus, it is clear that there is some overlapping of the noise and the signal spectra, although their main spectra are widely separated, 0 - 0.75 Hz versus 1.25 - 3 Hz.

The filter which is employed here is the zero phase bandpass filter with cosine tapering at both ends, as shown schematically in Figure III-12. The cut-off and corner frequencies at the low and high ends of the filters are represented as f_{LO}, f_L, and f_H, f_{HO}, respectively. Three groups of filters are used here. Their characteristic frequencies, f_{LO}, f_L, f_H, and f_{HO} are given in Table III-6. The first group is the highpass filter with varying low frequency cut-off. This is intended to show the effect of reducing the noise which mostly is in the low frequency. The second group is the lowpass filter with varying high frequency cut-off. This is to show the effect of the minor change in the signal spectral shape. The last group is the bandpass filter to show the combined effect of the noise reduction and the minor alteration of the signal spectral shape.

The typical results are presented here for the synthetic signal given by equation (III-3) with SNR = 18 dB. Figures III-13 through III-19 show the results using the first group of filters. For each figure, the cepstrum and the amplitude spectrum of the filtered signal, $x_{SN}^{F}(n)$, are given first, followed by the waveforms of the filtered signal and the cepstrum resolved

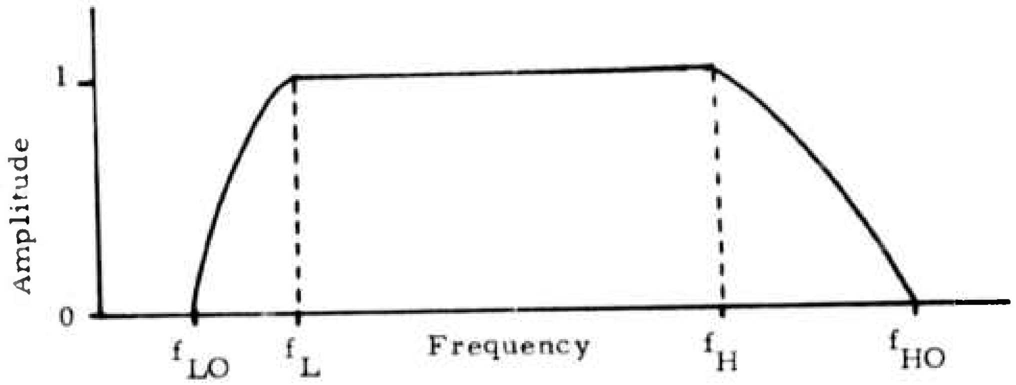

FIGURE III-12

RESPONSE OF THE BANDPASS FILTER

TABLE III-6

SPECIFICATIONS OF THE BANDPASS FILTERS

Group I. D.		f_{LO} (Hz)	f_L (Hz)	f_H (Hz)	f_{HO} (Hz)
I	1	0.001	0.1	5.0	5.0
	2	0.1	0.3	5.0	5.0
	3	0.3	0.5	5.0	5.0
	4	0.5	0.75	5.0	5.0
	5	0.75	1.0	5.0	5.0
	6	1.0	1.25	5.0	5.0
	7	1.25	1.5	5.0	5.0
II	1	0.001	0.1	4.5	5.0
	2	0.001	0.1	4.0	4.5
	3	0.001	0.1	3.5	4.0
	4	0.001	0.1	3.0	3.5
	5	0.001	0.1	2.5	3.0
III	1	0.75	1.0	3.0	3.5

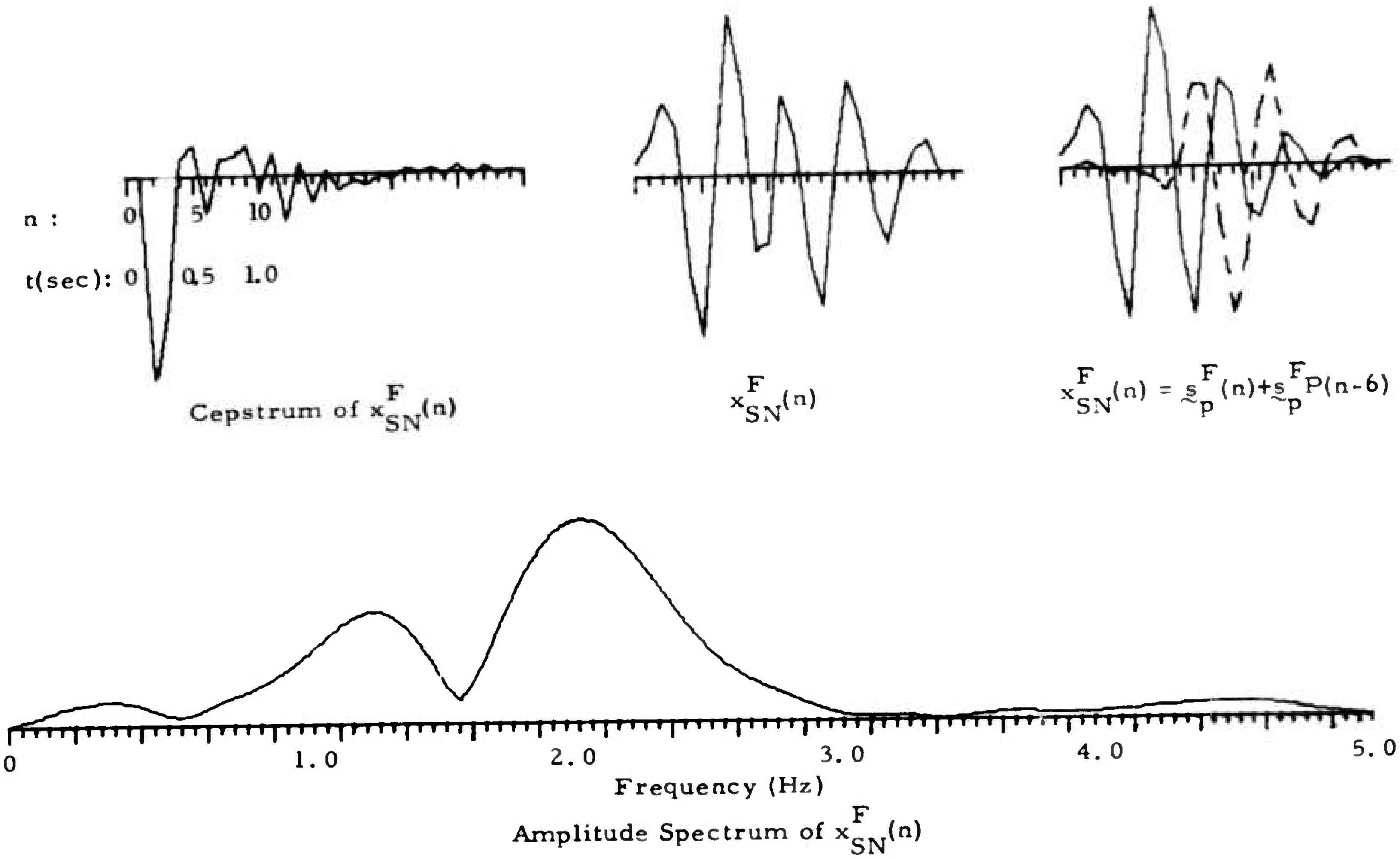

FIGURE III-13

CEPSTRUM ANALYZED RESULTS: PREFILTERING WITH FILTER I-1

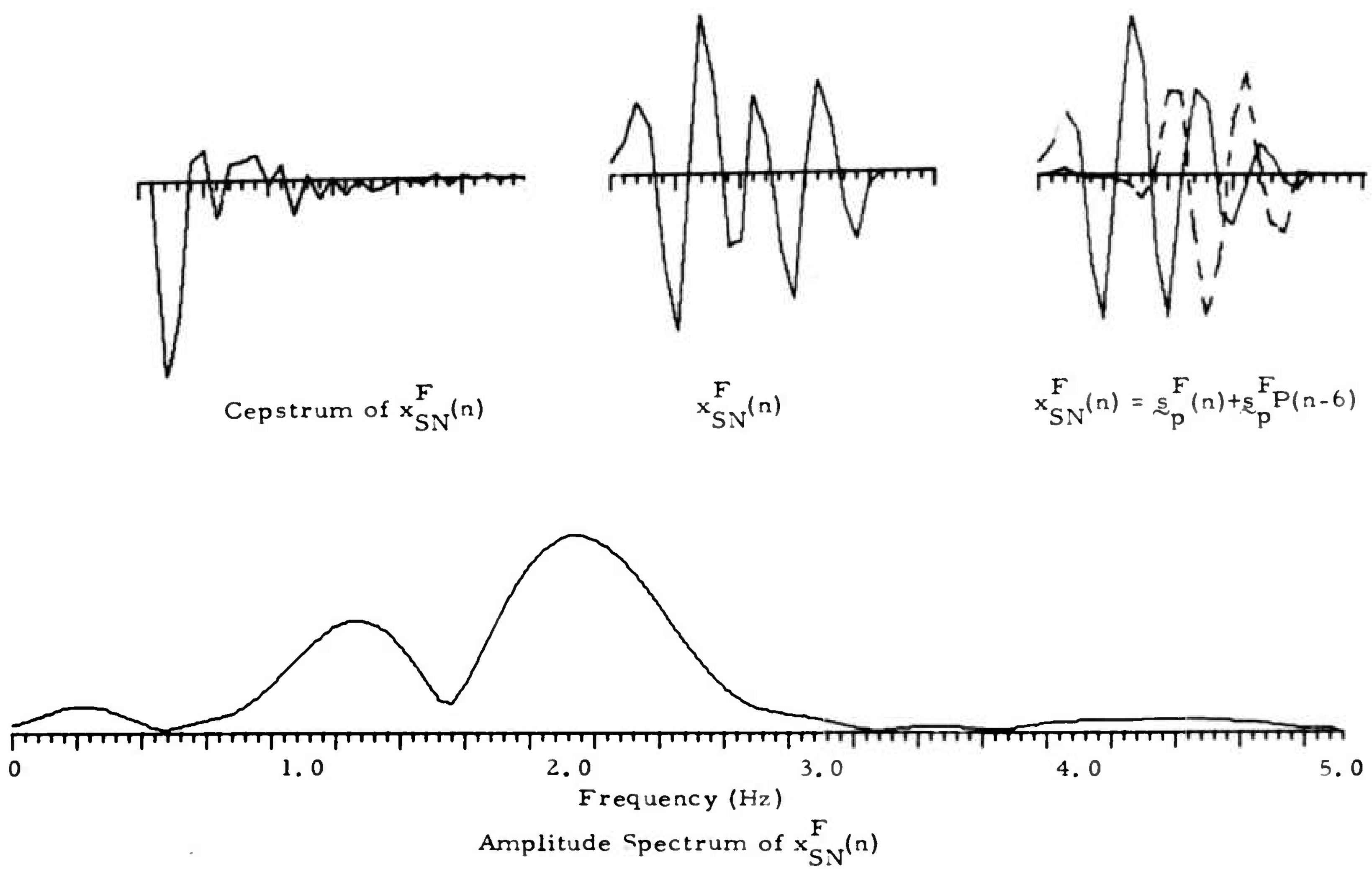

FIGURE III-14

CEPSTRUM ANALYZED RESULTS: PREFILTERING WITH FILTER I-2

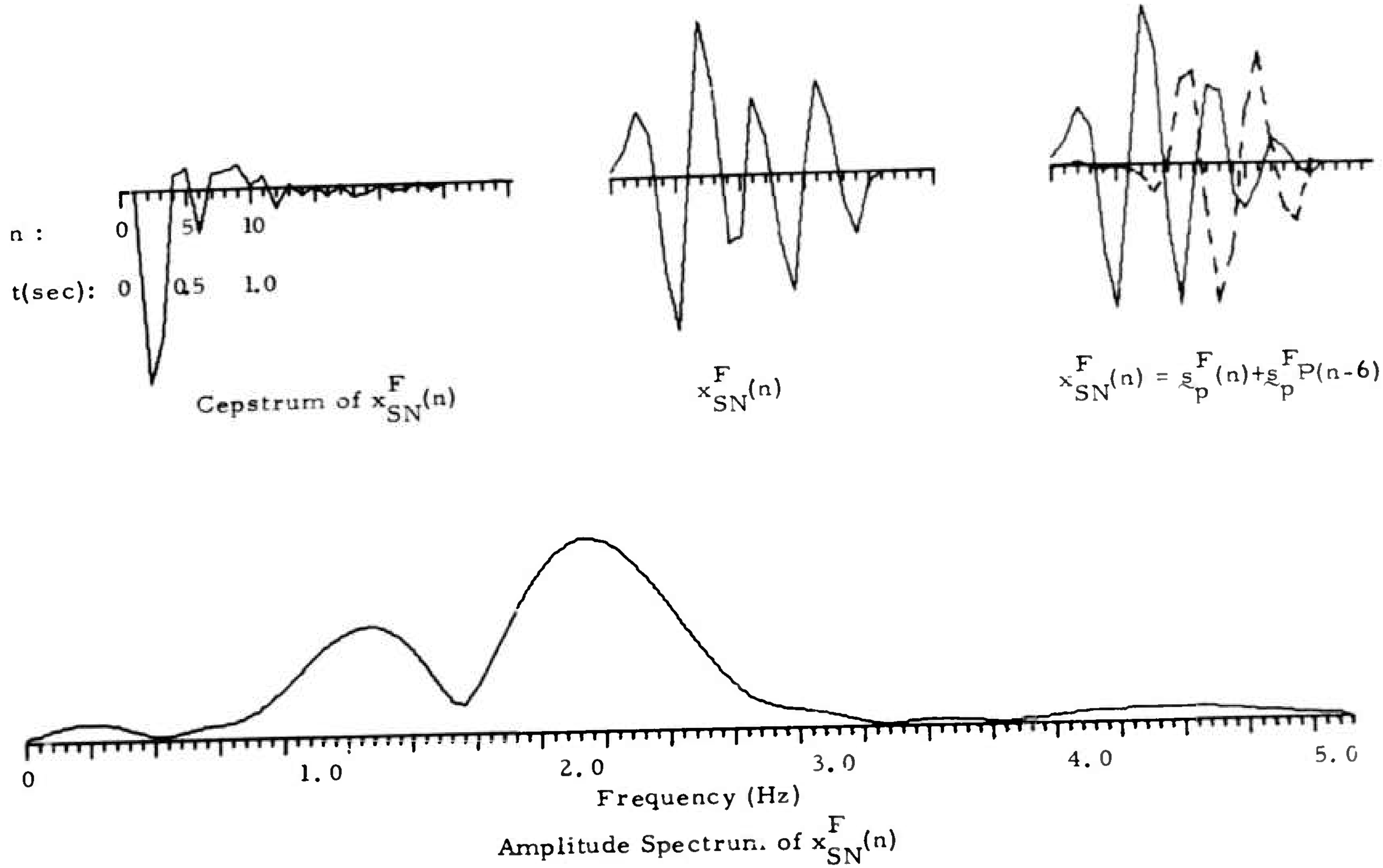

FIGURE III-15

CEPSTRUM ANALYZED RESULTS: PREFILTERING WITH FILTER I-3

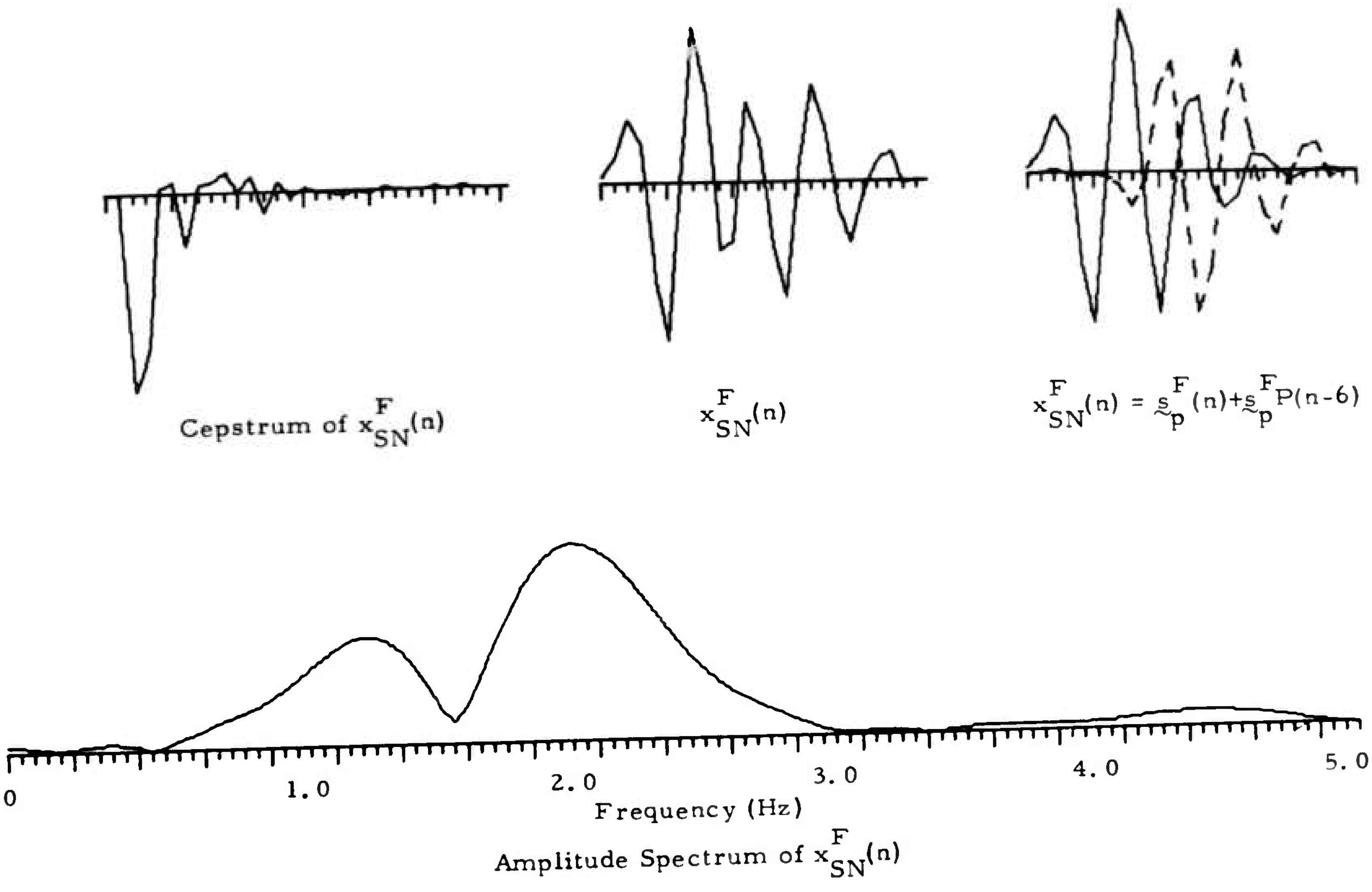

FIGURE III-16

CEPSTRUM ANALYZED RESULTS: PREFILTERING WITH FILTER I-4

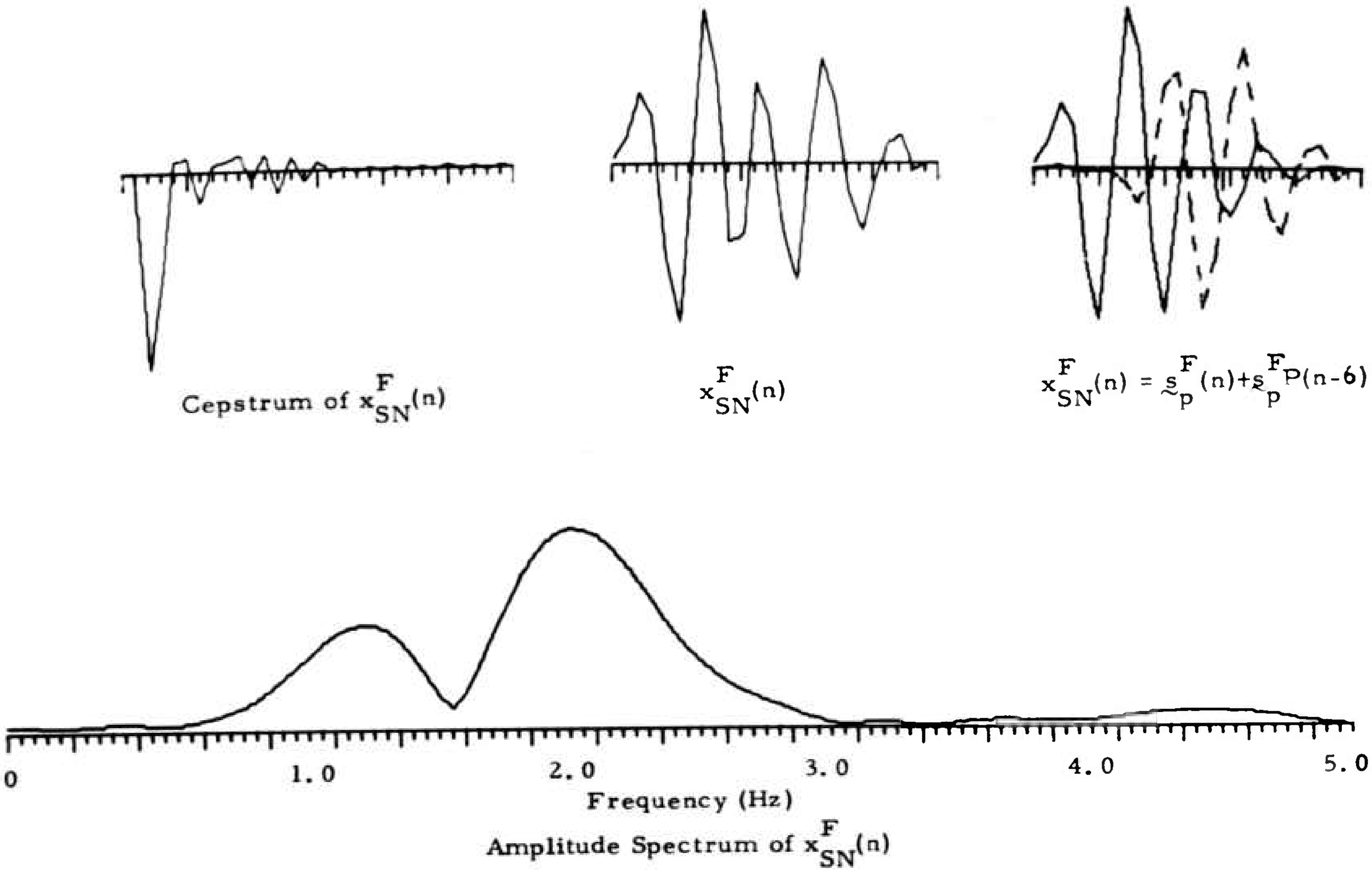

FIGURE III-17

CEPSTRUM ANALYZED RESULTS: PREFILTERING WITH FILTER I-5

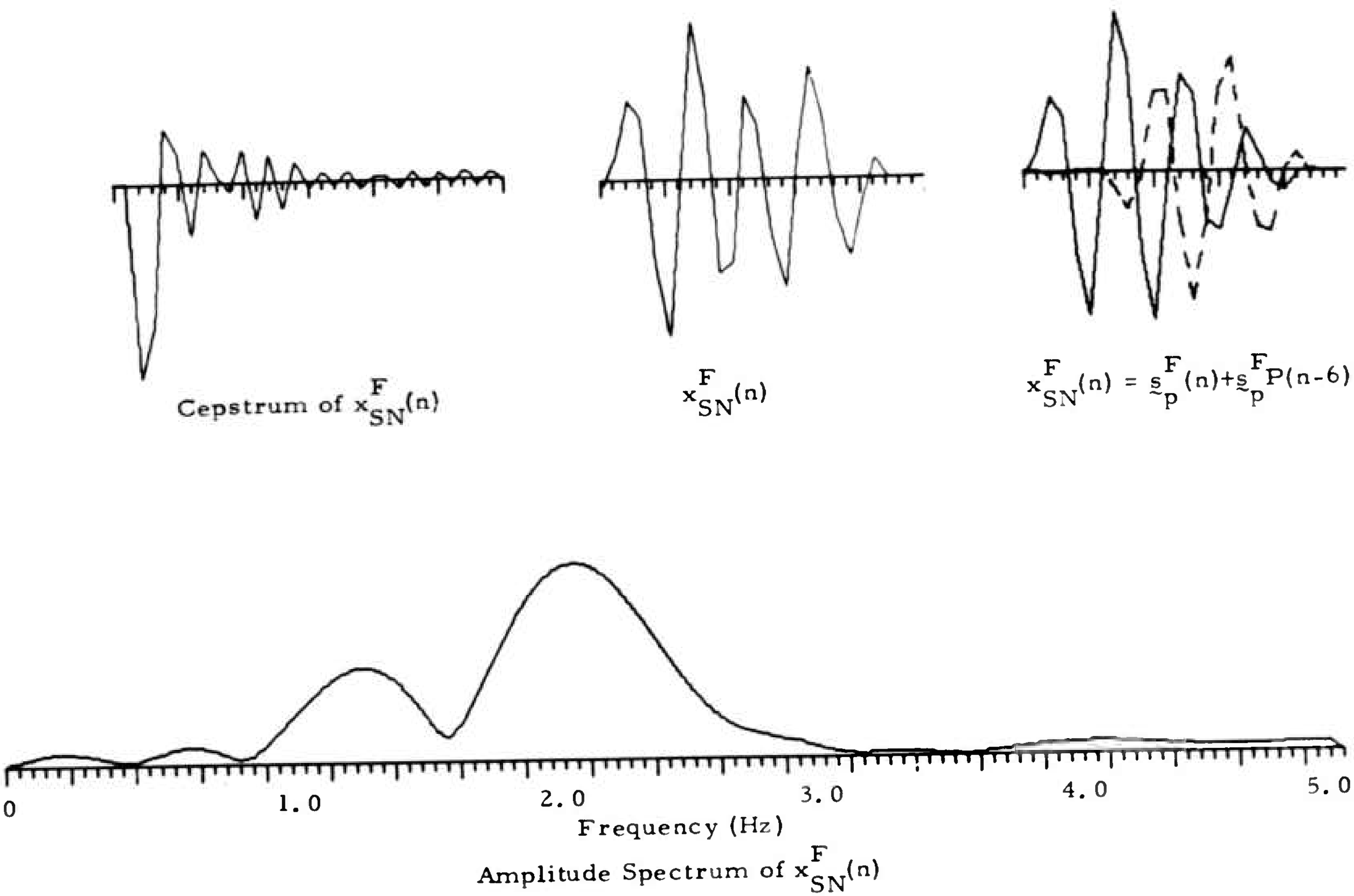

FIGURE III-18

CEPSTRUM ANALYZED RESULTS: PREFILTERING WITH FILTER I-6

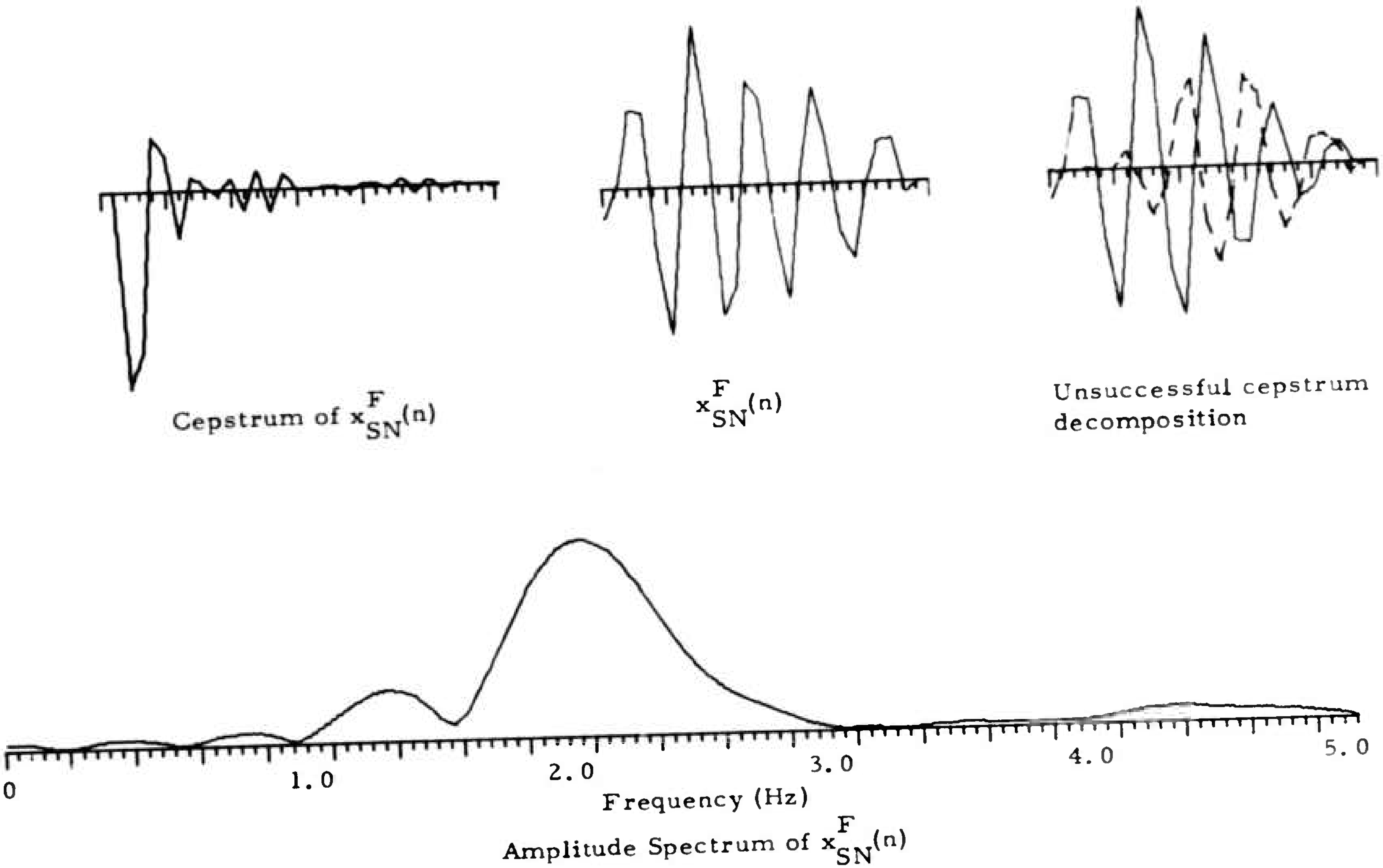

FIGURE III-19

CEPSTRUM ANALYZED RESULTS: PREFILTERING WITH FILTER I-7

signals, $\underset{\sim}{s}_p^F(n)$ and $\underset{\sim}{s}_p^F P(n - n_o)$. For comparison purposes, results without prefiltering are presented in Figure III-20. It is clear that no visible change in the waveform of the filtered signal is observed as compared to that of the unfiltered signal, except for the last filter whose f_{HO} and f_H get into the main part of the signal spectrum. However, from their amplitude spectra, we can see that the low frequency noise is reduced and the shape of the low frequency spectrum is deformed. Nevertheless, the general shape of the spectrum, especially the occurrances of the spectral maxima and minima, remains very much the same for a low frequency cut-off up to 1.0 Hz. The cepstral peaks due to the P-pP delay time appear at the right cepstrum times ($n = 6k$, $k = 1,2,\ldots$) and can be identified. It is hard to judge if the detection of these cepstral peaks is better for the filtered signals. It is fair to say that the prefiltering with the low frequency cut-off up to 1.0 Hz neither improves nor downgrades the detection. Also, the cepstrum resolved signals of the filtered and the unfiltered signals are very much the same. When the lower end of the filter is moved up to 1.5 Hz, the waveform and the low frequency spectrum of the filtered signal differ significantly from those of the unfiltered signal. Although the first cepstral peak still appears at the right cepstrum time, the identification of the second cepstral peak, which is supposed to be at $n = 12$, can no longer be made.

Figures III-21 through III-25 present similar results using the second group of filters. It is noticed that there is a long, low level high frequency tail (3.5 Hz - 5 Hz) in the amplitude spectra of the unfiltered signal. Again, the waveforms of the filtered signals are all very similar to that of the unfiltered signals. However, when the high frequency cut-off is below 4.5 Hz some of this high frequency tail is eliminated, and the second cepstral peak due to the P-pP delay time is no longer there. Thus, even a very minor change of the signal spectrum will seriously affect the detection of the P-pP delay time.

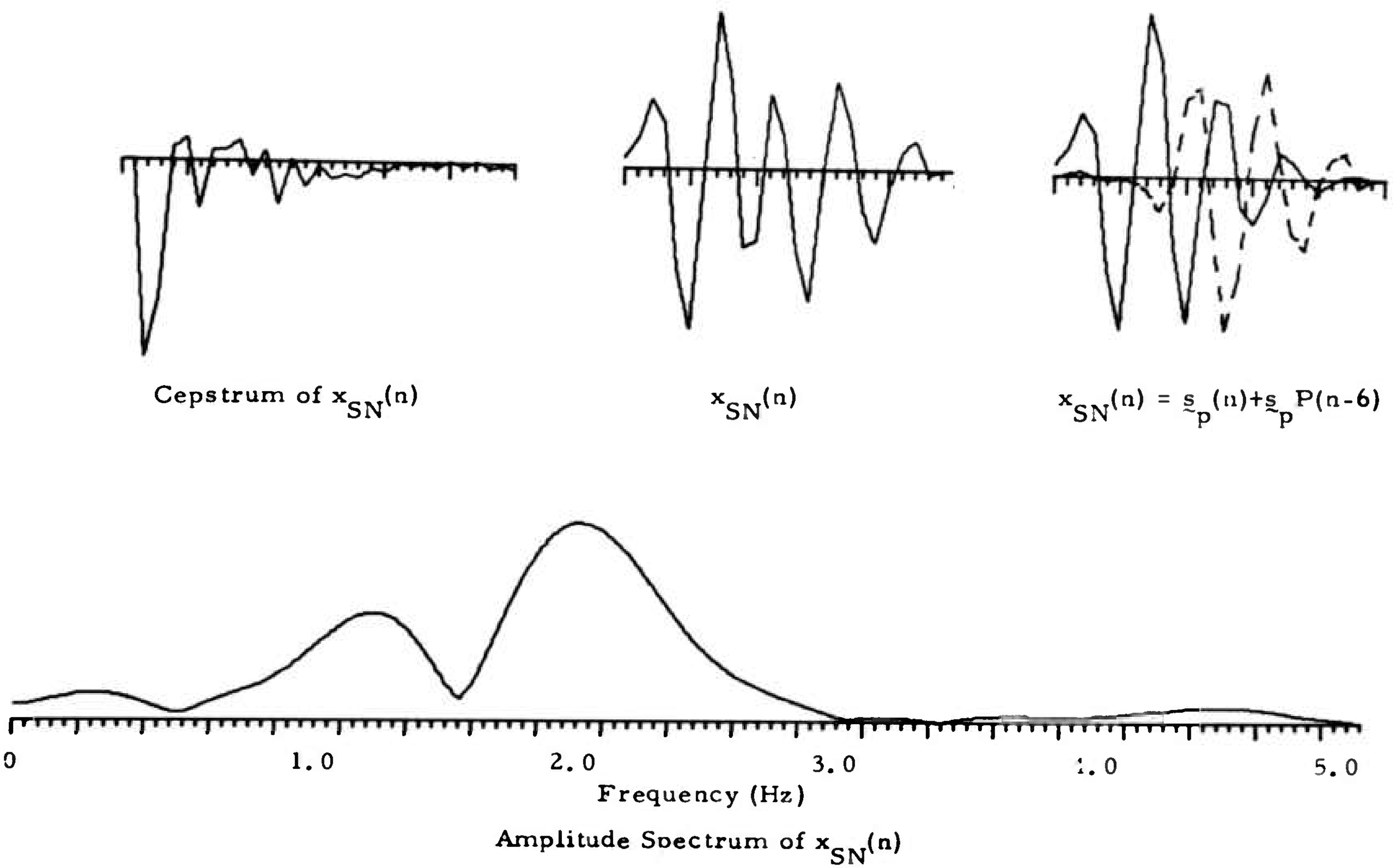

FIGURE III-20

CEPSTRUM ANALYZED RESULTS: NO PREFILTERING

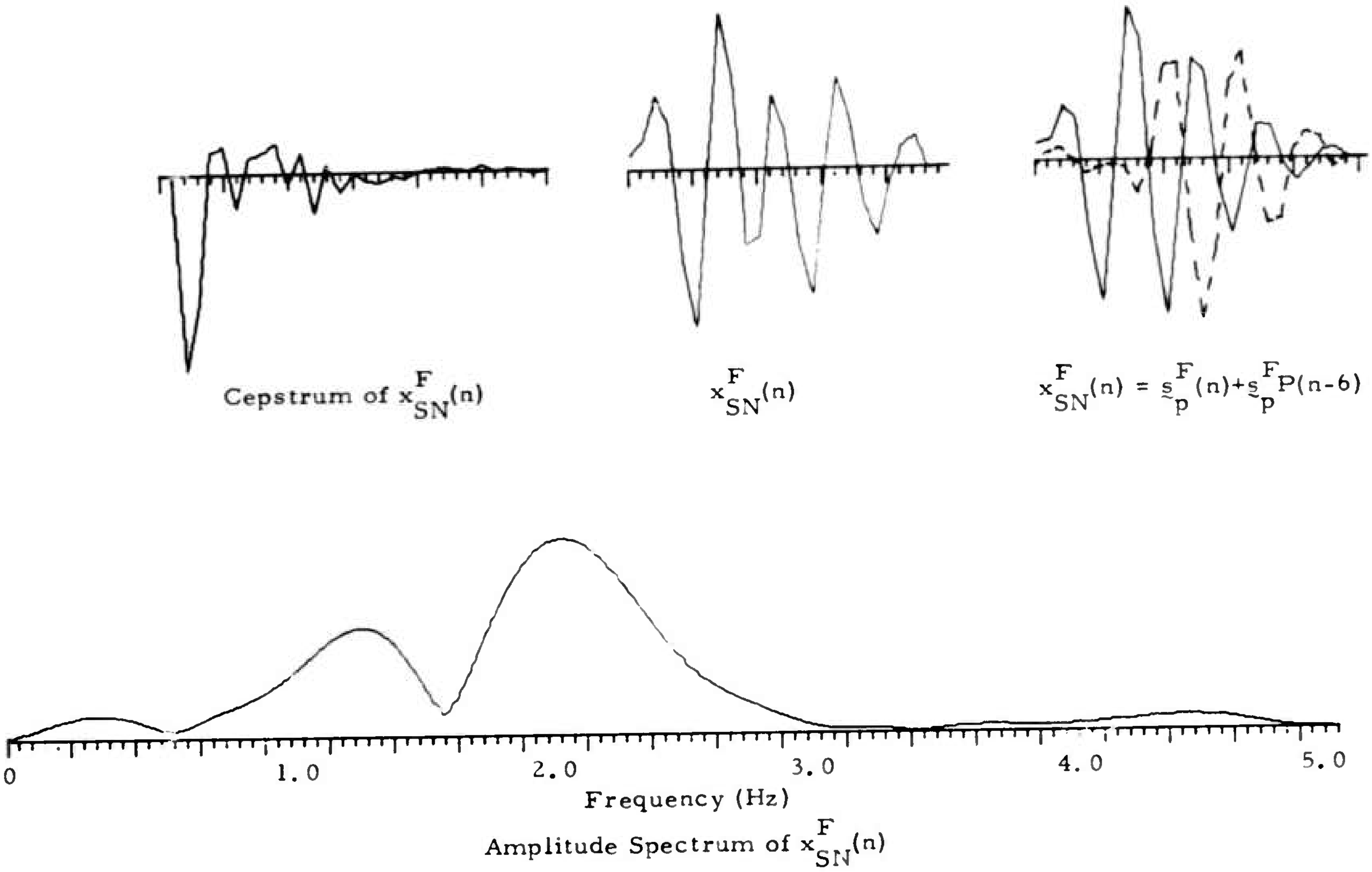

FIGURE III-21

CEPSTRUM ANALYZED RESULTS: PREFILTERING WITH FILTER II-1

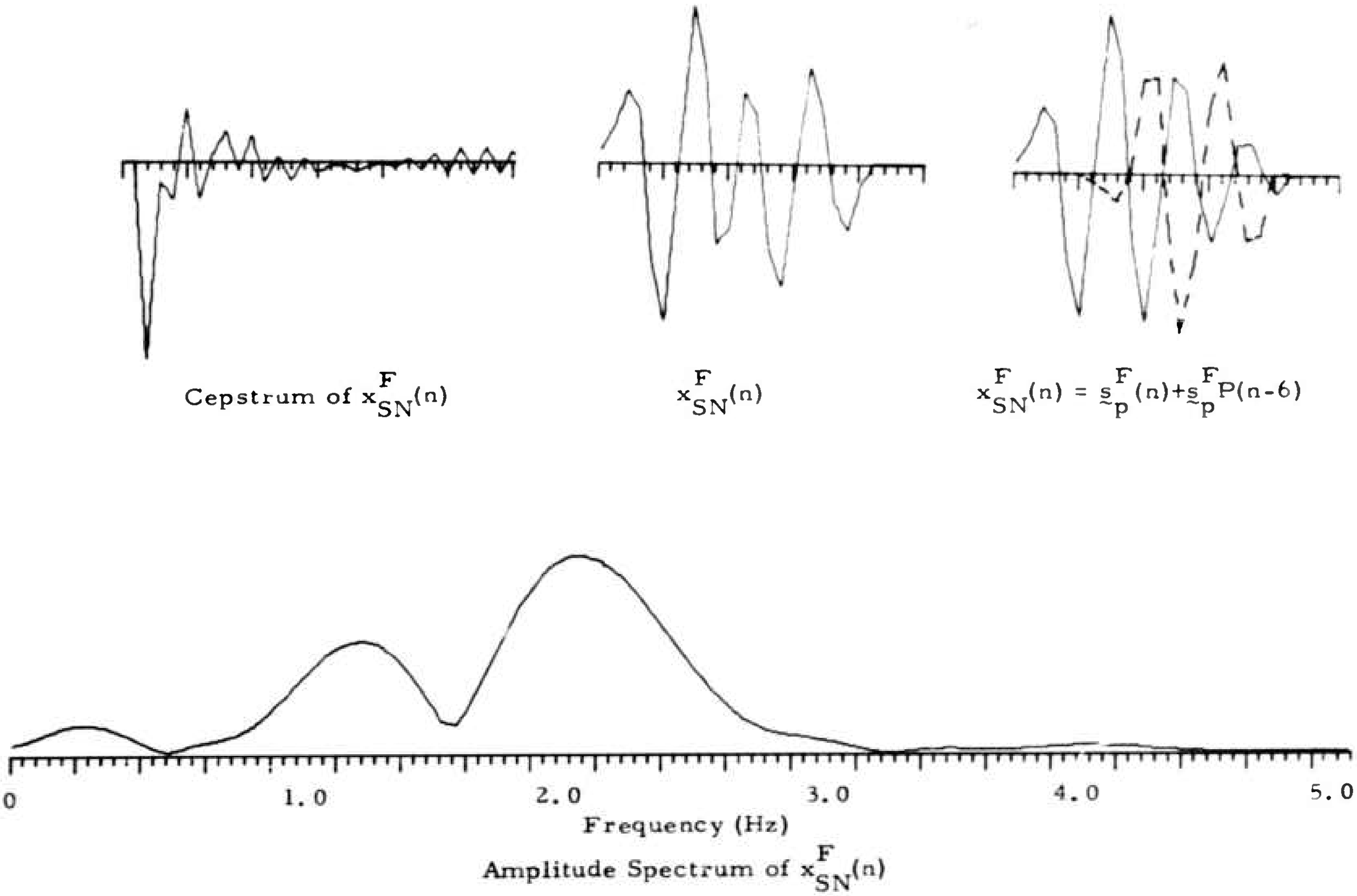

FIGURE III-22

CEPSTRUM ANALYZED RESULTS: PREFILTERING WITH FILTER II-2

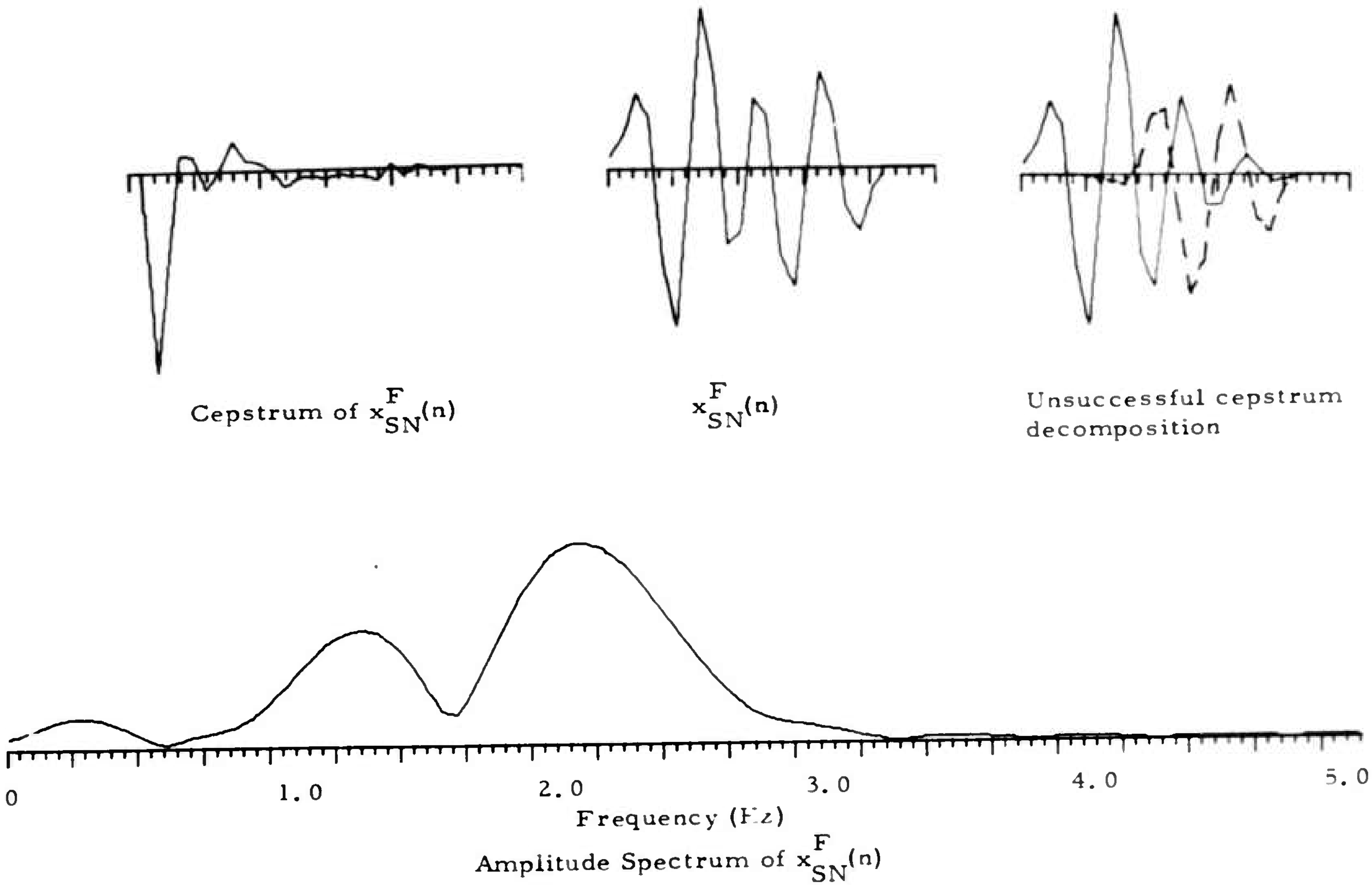

FIGURE III-23

CEPSTRUM ANALYZED RESULTS: PREFILTERING WITH FILTER II-3

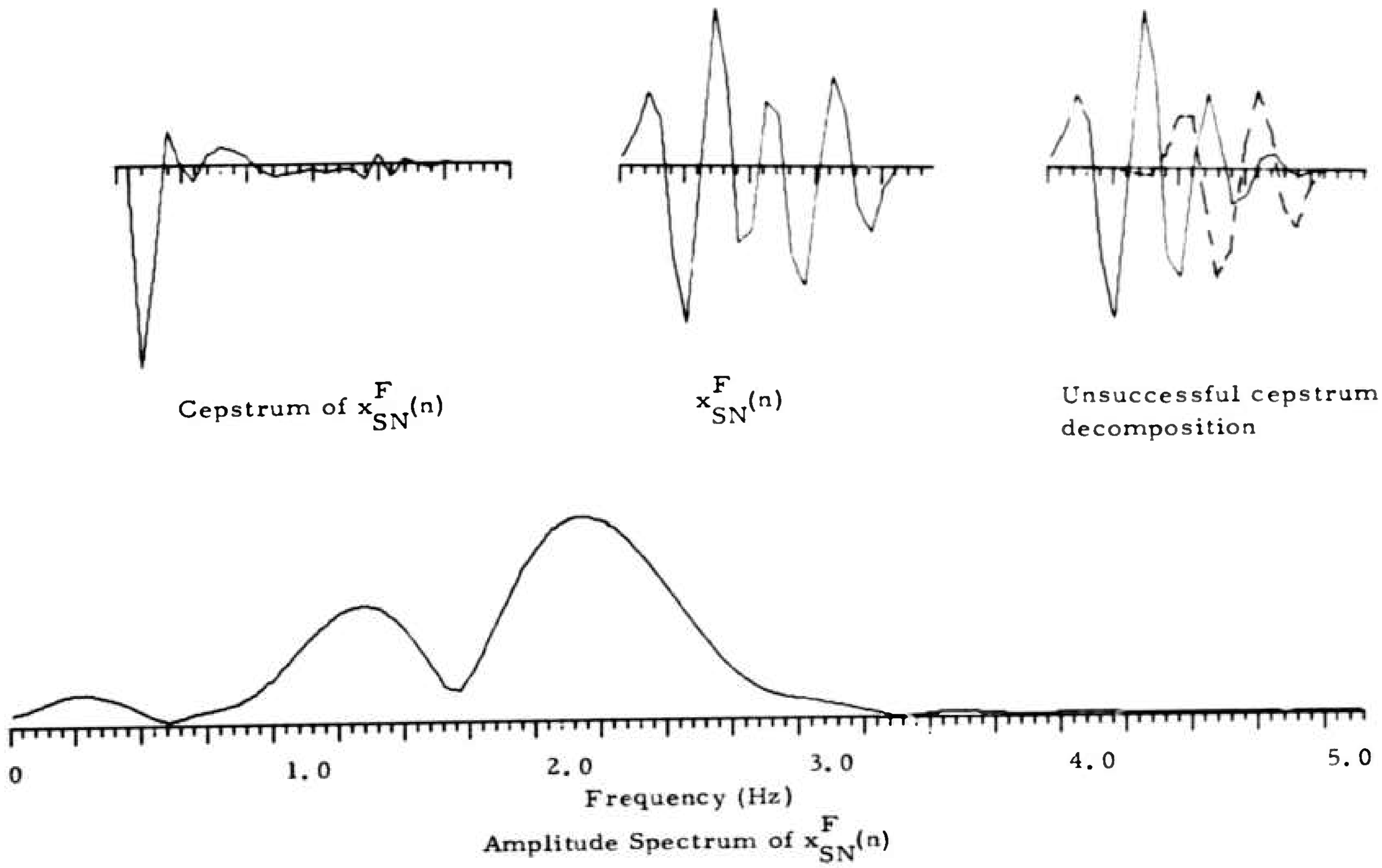

FIGURE III-24

CEPSTRUM ANALYZED RESULTS: PREFILTERING WITH FILTER II-4

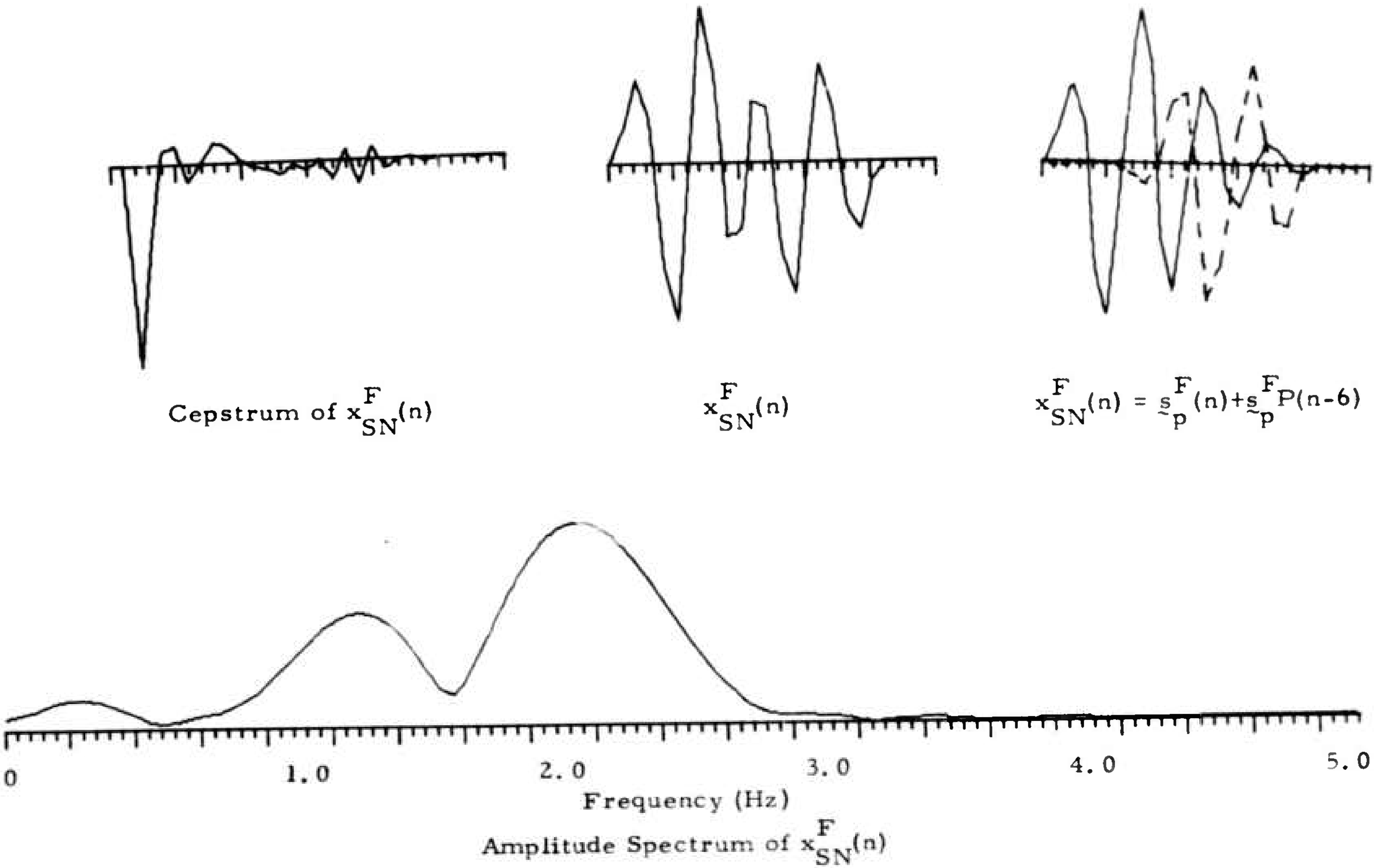

FIGURE III-25

CEPSTRUM ANALYZED RESULTS: PREFILTERING WITH FILTER II-5

The result for the last group is given in Figure III-26. This last filter only passes the main part of the signal spectrum. This simulates the normal operation of the bandpass filter to improve the signal-to-noise ratio. The waveform of the filtered signal again is very similar to that of the unfiltered signal, but the cepstrum analyzed results are worse than those for the second group. The cepstral peaks due to the P-pP delay time cannot be identified and the cepstrum decomposition is incorrect.

The major results from this study on the effect of prefiltering are as follows:

- Prefiltering with a bandpass filter does not affect the cepstrum analyzed results as long as the passband of the filter covers the entire signal spectrum.
- The reduction of the noise by prefiltering does not compensate the effect of minor distortion of the amplitude spectrum (associated with the prefiltering) on the detection of the P-pP delay time.

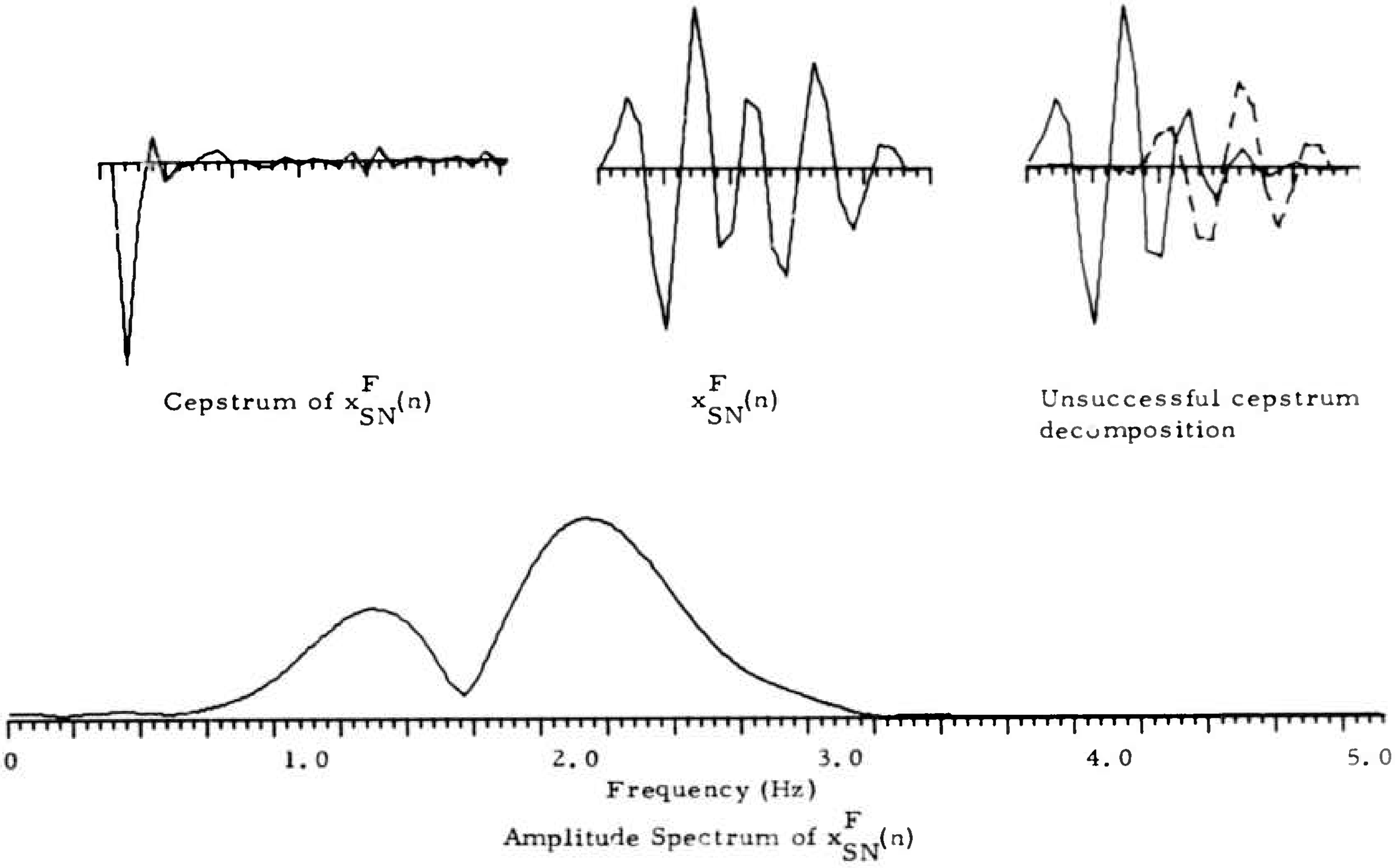

FIGURE III-26

CEPSTRUM ANALYZED RESULTS: PREFILTERING WITH FILTER III-1

SECTION IV

EXPERIMENTAL RESULTS: REAL SIGNALS

In this section cepstrum analysis is applied to several short-period P-waves from EKAZ events recorded at NORSAR. Table IV-1 presents source information for these events, including the calculated signal-to-noise ratio. The signal-to-noise ratios for these events range from 10 dB to 40 dB.

Before applying the cepstrum analysis to these signals, it is desirable to set up some criteria for judging the results. To facilitate the statements of these criteria, let us assume that the signal $x(n)$ is cepstrum decomposed into two resolved signals as follows:

$$x(n) = \underset{\sim}{s}_1(n) + \underset{\sim}{s}_2(n - \underset{\sim}{n}_o).$$

A real signal will be said to be successfully decomposed by the cepstrum analysis if:

(1) $\underset{\sim}{s}_1(n)$ and $\underset{\sim}{s}_2(n - \underset{\sim}{n}_o)$ resemble a relistic teleseismic short-period P-phase of a single underground explosion (i.e., if they are simple and have reasonably finite trace lengths). Also, the first few significant amplitude peaks of $\underset{\sim}{s}_2(n - \underset{\sim}{n}_o)$ should be delayed by $\underset{\sim}{n}_o$ samples with respect to the corresponding peaks of $\underset{\sim}{s}_1(n)$; and if $\underset{\sim}{s}_2$ is the surface reflection of $\underset{\sim}{s}_1$, they should be of opposite sign.

(2) $\underset{\sim}{s}_1(n) \approx 0$ for $n > N_1$, where N_1 is a reasonably finite integer (for the EKAZ events recorded at NORSAR, $N_1 \approx 1.5\text{-}2.0$ seconds).

TABLE IV-1

PRESUMED UNDERGROUND EXPLOSIONS IN EASTERN KAZAKH

Event I. D.	Date	Location		m_b	SNR
		Latitude	Longitude		
EKZ/159/01N	06/07/72	49.8	78.2	5.5	39
KAZ/081/04N	03/22/71	49.7	78.2	5.8	34
EKZ/239/03N	08/26/72	50.0	77.8	5.5	33
KAZ/170/04N	06/19/71	50.0	79.1	5.5	30
EKZ/333/06N	11/29/71	49.8	78.1	5.5	28
KAZ/282/06N	10/09/71	50.0	77.7	5.4	22
EKZ/246/08N	09/02/72	50.0	77.7	5.1	14
EKZ/363/04N	12/28/72	50.0	78.0	4.5	10

(3) $\underset{\sim}{s}_2(n - \underset{\sim}{n}_o) \approx 0$ for $n < \underset{\sim}{n}_o$.

Figures IV-1 through IV-8 present the results of cepstrum analyzing these signals. For each figure, the waveform and the cepstrum of the signal are displayed, together with the cepstrum resolved P-phase (solid line) and the pP-phase (dashed line). By examining these cepstra, even for those high SNR events, we cannot find the periodic occurrances of the cepstral peaks due to the P-pP delay time as that discussed in Subsection III-B. This is thought to be reasonable, since in general the surface reflected pP-phase is not the exact replica of the direct P-phase. However, it is noticed that, except for two low SNR events, the appearances of these cepstra are similar to those demonstrated in Subsection III-C, where the synthetic signal consisted of two non-identical signals. Thus, for the real signals, to obtain the estimate of the possible P-pP delay time, the successful decomposition of these signals must be achieved first as mentioned in Subsection III-C.

Since the cepstrum does not show the definite peaks due to the possible P-pP delay time, the most straightforward way to filter the cepstrum is to apply the shortpass filter at every cepstral peak which is suspected to be the cepstral peak due to the P-pP delay time. Then the corresponding cepstrum resolved signals are examined to see if the signal is successfully decomposed. As an example, consider the event EKZ/333/06N as shown in Figure IV-5. The cepstral peaks at $n = 5, 6, 7, 8,$ and 10 are decided to be the suspicious peaks. The cepstrum decomposition by applying the shortpass filter at $n = 7$ is shown in Figure IV-5a and is judged unsuccessful. The same conclusion is made for $n = 8$ and 10. The cepstrum resolved signals shown in Figure IV-5 are obtained by applying the shortpass filter at $n = 6$. The similar successful decomposition is also achieved by filtering at $n = 5$. The P-pP delay time is estimated to be 0.6 seconds.

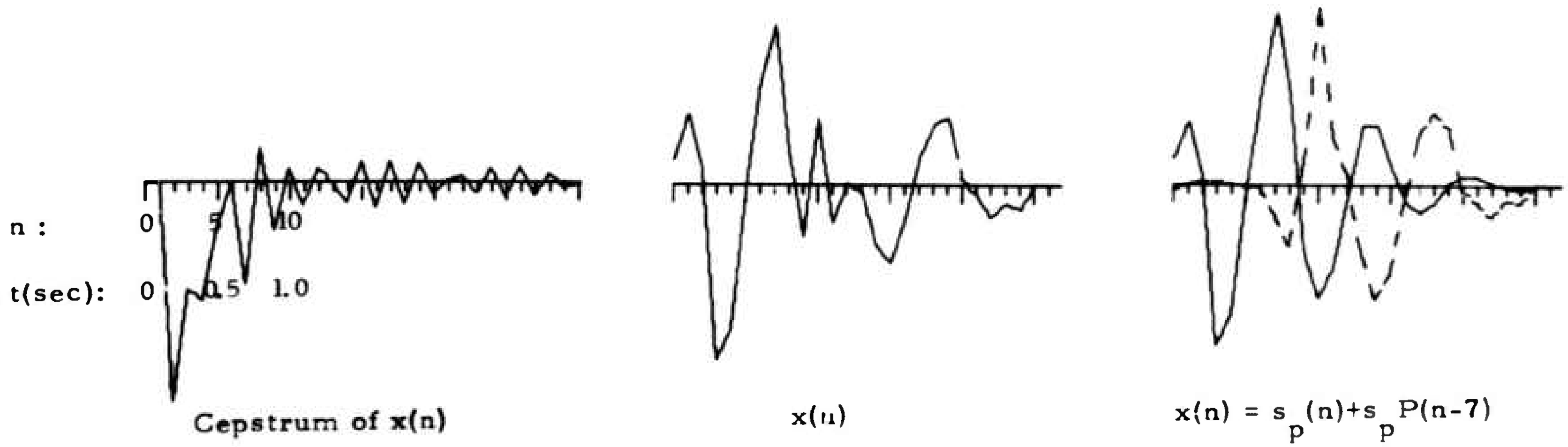

FIGURE IV-1

CEPSTRUM ANALYZED RESULTS: EKZ/159/01N

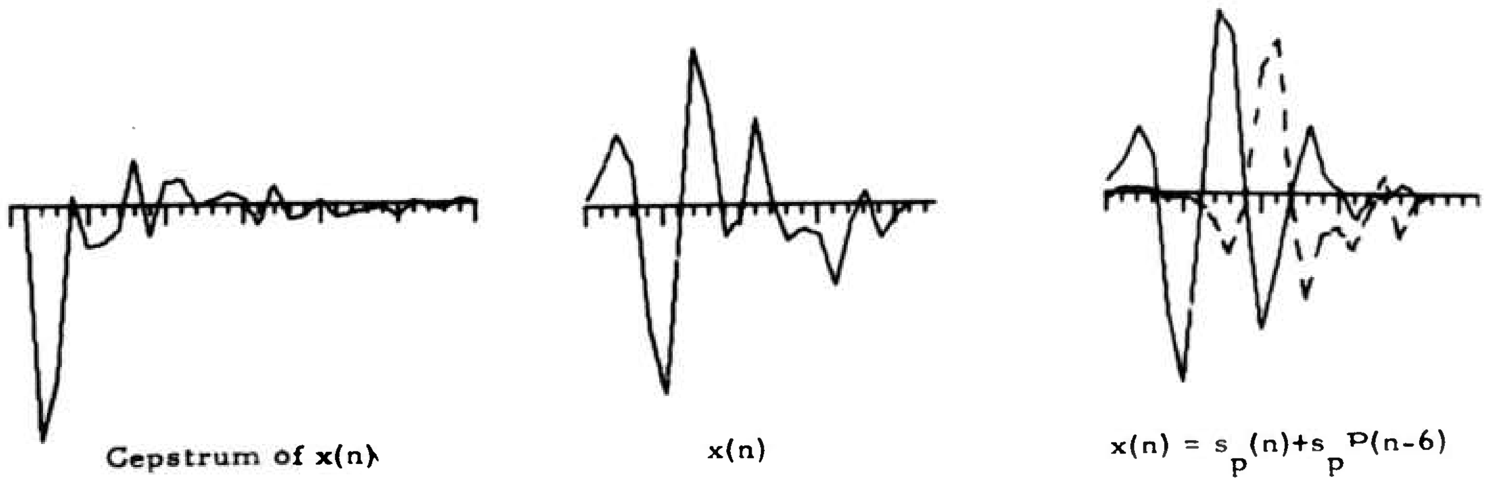

FIGURE IV-2

CEPSTRUM ANALYZED RESULTS: KAZ/081/04N

FIGURE IV-3

CEPSTRUM ANALYZED RESULTS: EKZ/239/03N

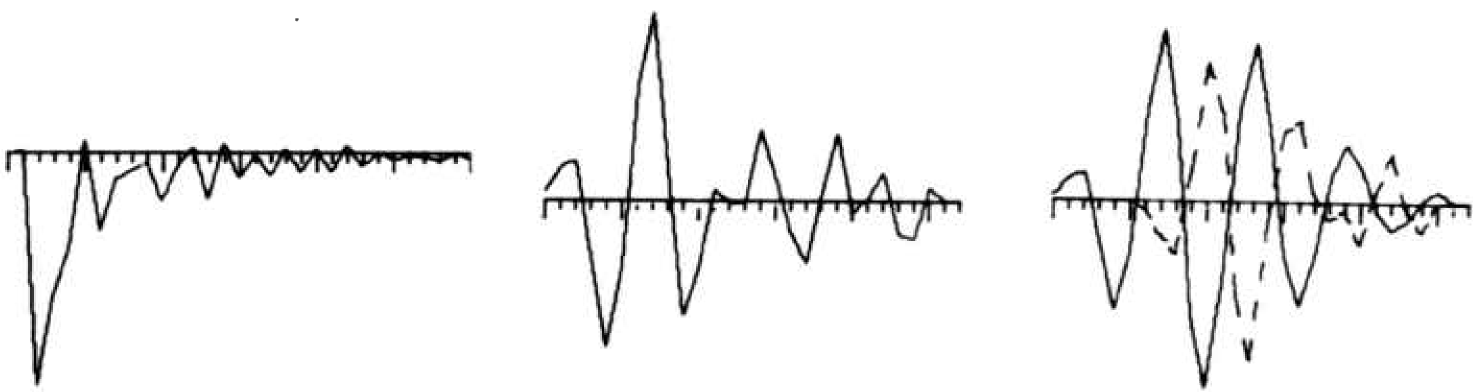

FIGURE IV-4

CEPSTRUM ANALYZED RESULTS: KAZ/170/04N

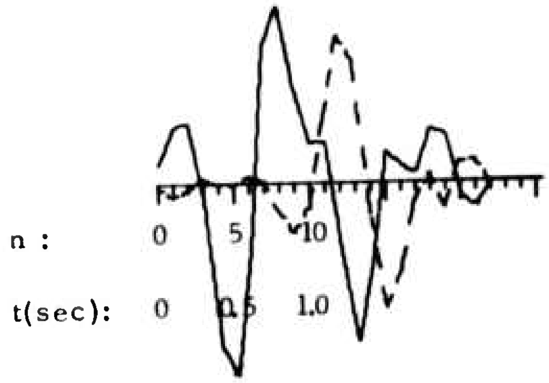

FIGURE IV-5a

CEPSTRUM RESOLVED SIGNALS: SHORTPASS FILTER AT n = 7 FOR EKZ/333/06N

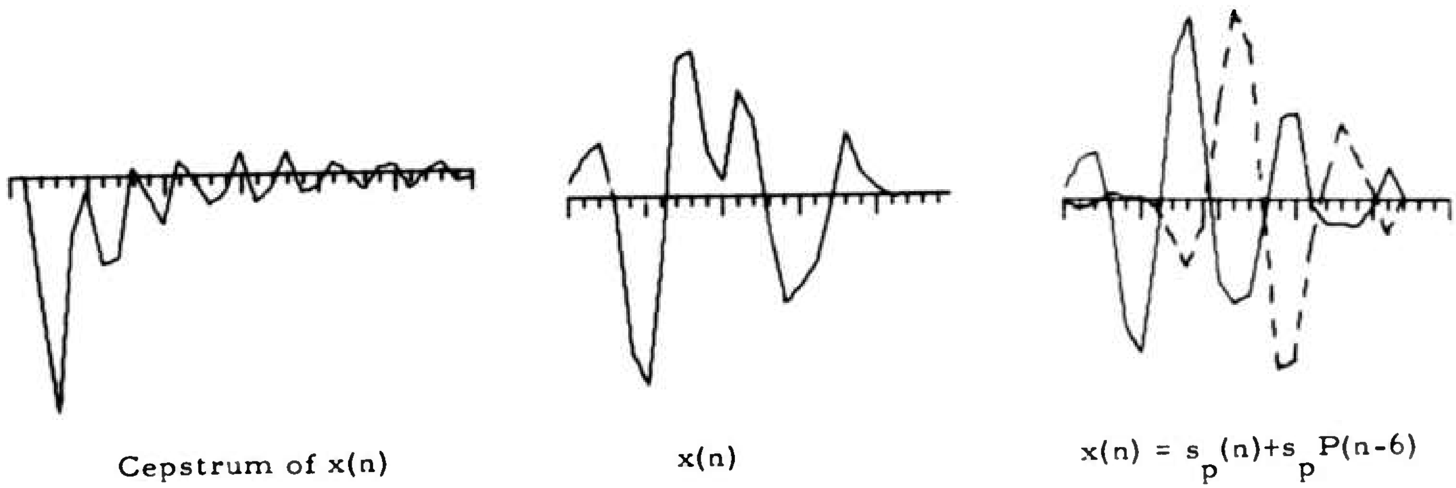

FIGURE IV-5b

CEPSTRUM ANALYZED RESULTS: EKZ/333/06N

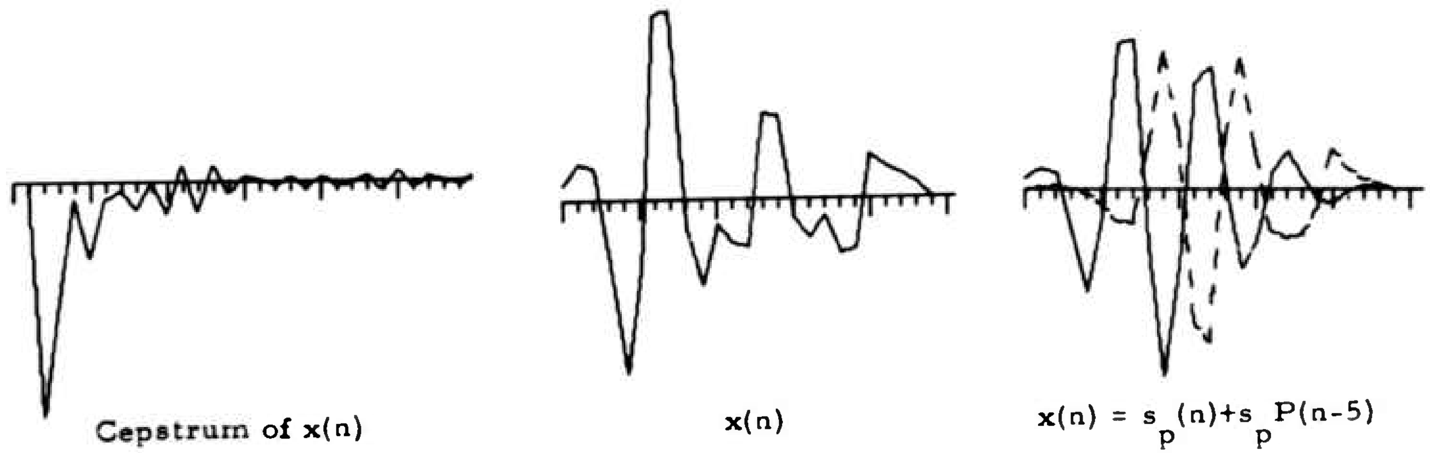

FIGURE IV-6

CEPSTRUM ANALYZED RESULTS: KAZ/282/06N

Cepstrum of x(n) | x(n) | $x(n) = s_p(n) + s_p P(n-6)$

FIGURE IV-7

CEPSTRUM ANALYZED RESULTS: EKZ/246/08N

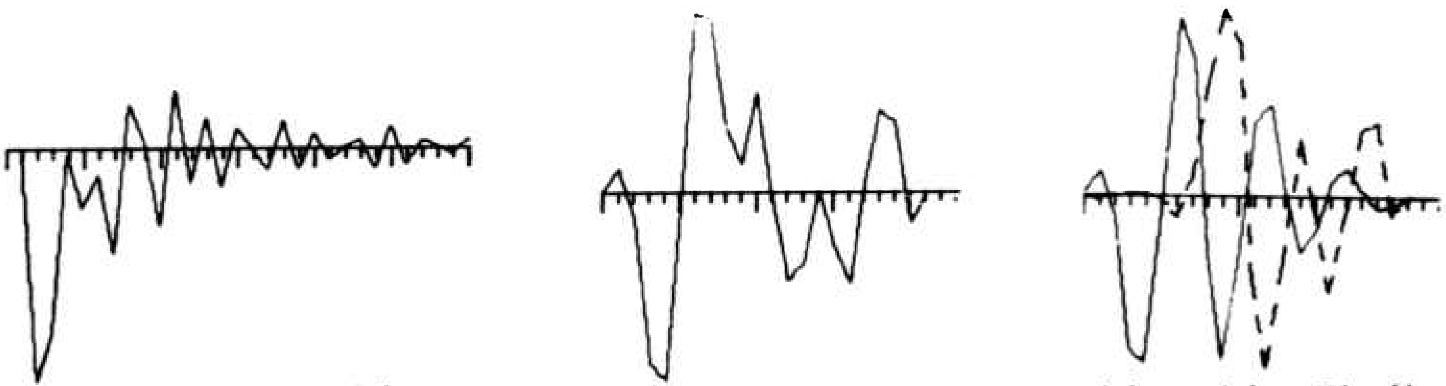

Cepstrum of x(n) | x(n) | $x(n) = s_p(n) + s_p P(n-6)$

FIGURE IV-8

CEPSTRUM ANALYZED RESULTS: EKZ/363/04N

The final cepstrum decompositions of these signals are expressed in the form like equation (III-6) and are given in Table IV-2. Also shown are the similarity coefficient and the amplitude ratio of the resolved signals. It is noticed that these similarity coefficients range from 0.7 to 0.9 which are compatible with those of the synthetic signals used in Subsection III-C. However, the trend relation of increasing similarity with increasing signal-to-noise ratio, which has been found in Subsection III-B for the synthetic signal with identical P-phase and pP-phase, is not observed here.

TABLE IV-2

FINAL CEPSTRUM DECOMPOSITIONS OF EKAZ EVENTS

Event I. D.	Cepstrum Decomposition	a (1)	ρ (2)
EKZ/159/01N	$x(n) = s_p(n) + s_pP(n-7)$	0.87	0.864
KAZ/081/04N	$x(n) = s_p(n) + s_pP(n-6)$	0.74	0.712
EKZ/239/03N	$x(n) = s_p(n) + s_pP(n-5)$	0.60	0.690
KAZ/170/04N	$x(n) = s_p(n) + s_pP(n-6)$	0.83	0.796
EKZ/333/06N	$x(n) = s_p(n) + s_pP(n-6)$	1.05	0.906
KAZ/282/06N	$x(n) = s_p(n) + s_pP(n-5)$	0.85	0.874
EKZ/246/08N	$x(n) = s_p(n) + s_pP(n-6)$	0.65	0.749
EKZ/363/04N	$x(n) = s_p(n) + s_pP(n-5)$	1.03	0.730

(1) a : peak-to-peak amplitude ratio of $s_pP(n)$ and $s_p(n)$

(2) ρ : similarity coefficient of $s_p(n)$ and $s_pP(n)$

SECTION V

CONCLUSIONS

The noise, the dissimilarity between the P-phase and the pP-phase, and the prefiltering are found to produce various unfavorable effects on the detection of the P-pP delay time and the successful cepstrum analysis of the mixed P- and pP-wave. The dissimilarity will affect the detection more seriously than the noise does. The increase of the noise level will only gradually obscure the cepstral peaks due to the P-pP delay time, while the dissimilarity completely destroys the periodic occurrances of these cepstral peaks. For the identical P-phase and the pP-phase, the cepstrum analysis can detect the P-pP delay time as short as 0.4 second and successfully recover them for the signal-to-noise ratio as low as 12 dB. For the non-identical P-phase and pP-phase, the cepstrum analysis can still achieve the successful decomposition for the similarity coefficient about 0.55. This, in turn, can be used to estimate the P-pP delay time.

In reality, the pP-phase and the P-phase are not identical, although they can be expected to be quite similar. Therefore, for the real mixed P- and pP-wave, we should not expect to find the periodicity of the cepstral peaks due to the P-pP delay time. Rather, we should look for the suspicious cepstral peaks and filter the cepstrum accordingly for the possible decomposition. The correct estimate of the P-pP delay time can only be obtained through the successful cepstrum decomposition of the mixed signal.

Prefiltering, in general, does not affect the cepstrum analyzed results as long as the passband of the filter covers the entire signal spectrum. However, it is suggested that the prefiltering should be avoided if the signal-to-noise ratio is not unreasonably low.

SECTION VI

REFERENCES

Bakum, W. H., and L. R. Johnson, 1973, The Deconvolution of Teleseismic P Waves From Explosions MILROW and CANNIKIN, Geophys. J. R. Astr. Socl, 34, pp 321-342.

Churchill, R. V., 1960, Complex Variable and Applications, McGraw-Hill Book Company, New York.

Harley, T. W., 1971, Long Period Array Processing Development, Final Report, Equipment Group, Texas Instruments Incorporated, Dallas, Texas.

Lane, S. S., and D. Sun, 1974a, Counterevasion Studies, Semi-Annual Technical Report No. 2-Part B, Equipment Group, Texas Instruments Incorporated, Dallas, Texas.

Lane, S. S., and D. Sun, 1974b, Counterevasion Studies, Semi-Annual Technical Report No. 3-Part B, Equipment Group, Texas Instruments Incorporated, Dallas, Texas.

Schafer, R. W., 1969, Echo Removal by Discrete Generalized Linear Filtering, Technical Report 466, Research Laboratory of Electronics, Massachusetts Institute of Technology, Cambridge, Massachusetts.

Ulrych, T. J., 1971, Application of Homomorphic Deconvolution to Seismology, Geophysics, 36, pp 650-660.

Ulrych, T. J., O. G. Jensen, R. M. Ellis, and P. G. Somervill, 1972, Homomorphic Deconvolution of Some Teleseismic Events, Bull. Seis. Soc. Am., 62, pp 1269-1281.

UNCLASSIFIED

SECURITY CLASSIFICATION OF THIS PAGE (When Data Entered)

REPORT DOCUMENTATION PAGE

READ INSTRUCTIONS BEFORE COMPLETING FORM

1. REPORT NUMBER: AFOSR - TR - 76 - 1064
2. GOVT ACCESSION NO.:
3. RECIPIENT'S CATALOG NUMBER:
4. TITLE (and Subtitle): COUNTEREVASION STUDIES - THE EFFECTS OF NOISE, DISSIMILARITY, AND PREFILTERING ON CEPSTRUM ANALYSIS.
5. TYPE OF REPORT & PERIOD COVERED: Semi-Annual Technical
6. PERFORMING ORG. REPORT NUMBER: TI-ALEX(02)-TR-75-02-PART-B
7. AUTHOR(s): David Sun
8. CONTRACT OR GRANT NUMBER(s): F44620-73-C-0055, ARPA Order-1827
9. PERFORMING ORGANIZATION NAME AND ADDRESS: Texas Instruments Incorporated, Equipment Group, Dallas, Texas 75222
10. PROGRAM ELEMENT, PROJECT, TASK AREA & WORK UNIT NUMBERS: ARPA Program Code No. F10
11. CONTROLLING OFFICE NAME AND ADDRESS: Advanced Research Projects Agency, Nuclear Monitoring Research Office, Arlington, Virginia 22209 — 82p.
12. REPORT DATE: 30 November 1975
13. NUMBER OF PAGES: 80
14. MONITORING AGENCY NAME & ADDRESS (if different from Controlling Office): Air Force Office of Scientific Research /NP, Bolling Air Force Base, Bldg. 410, Washington, D.C. 20332
15. SECURITY CLASS. (of this report): UNCLASSIFIED

15a. DECLASSIFICATION/DOWNGRADING SCHEDULE:

16. DISTRIBUTION STATEMENT (of this Report)

APPROVED FOR PUBLIC RELEASE, DISTRIBUTION UNLIMITED

17. DISTRIBUTION STATEMENT (of the abstract entered in Block 20, if different from Report)

Semi-annual technical rept. no. 5, (pt. B), 1 May - 31 Oct 75,

18. SUPPLEMENTARY NOTES

TECH, OTHER

19. KEY WORDS (Continue on reverse side if necessary and identify by block number)

Seismology
Complex Cepstrum
Nuclear Explosions
Depth Phase
Noise
Dissimilarity
Prefiltering

20. ABSTRACT (Continue on reverse side if necessary and identify by block number)

The effects of the noise, the dissimilarity, and the prefiltering on the detection of the P-pP delay time and the successful decomposition of the mixed P- and -pP wave by employing the cepstrum analysis are studied here. These effects have been investigated by extracting the direct P-phases and the surface reflected pP-phases from several presumed underground explosions in eastern Kazakh, and remixing them at various time delays with the addition of various levels of the realistic seismic noise. The quality of the cepstrum

DD FORM 1 JAN 73 1473 EDITION OF 1 NOV 65 IS OBSOLETE

UNCLASSIFIED 405076

SECURITY CLASSIFICATION OF THIS PAGE (When Data Entered)

20. continued

analyzed results as a function of the signal-to-noise ratio, the delay time, and the dissimilarity between the P-phase and the pP-phase have been obtained for a number of such events. In general, it is found that the cepstrum analysis can detect the P-pP delay time as short as 0.4 second and successfully recover the P- and the pP-phases for the signal-to-noise ratio down to about 12 dB. When the similarity coefficient between the P- and the pP-phases is less than 1.0, the detection of the P-pP delay time becomes not so obvious as it is when they are identical. The dissimilarity between the P-phase and the pP-phase will affect the detection of the P-pP delay time more seriously than the noise in the cepstrum analysis. Prefiltering of the noisy mixed P- and -pP wave with the standard bandpass filter will not affect the cepstrum analyzed results as long as the filter band covers the entire signal spectrum; although it seems that no prefiltering will offer better detection of the P-pP delay time.